

[Click here to view linked References](#)

1  
2  
3  
4  
5  
6  
7  
8  
9  
10  
11  
12

**Plutonic xenoliths from Martinique, Lesser Antilles: evidence for open system processes  
and reactive melt flow in island arc crust**

13  
14  
15  
16  
17  
18  
19  
20  
21  
22  
23  
24  
25  
26  
27  
28  
29  
30  
31  
32  
33  
34

George F Cooper<sup>1\*</sup>, Jon P Davidson<sup>1</sup>, Jon D Blundy<sup>2</sup>

<sup>1</sup>Department of Earth Sciences, Durham University, Science Labs, Durham DH1 3LE

<sup>2</sup>School of Earth Sciences, University of Bristol, Wills Memorial Building, BS8 1RJ

\*corresponding author:

email: [george.cooper@durham.ac.uk](mailto:george.cooper@durham.ac.uk)

35  
36  
37  
38  
39  
40  
41  
42  
43  
44

**Keywords:** Lesser Antilles; Martinique; plutonic; xenoliths; amphibole; reactive melt

45  
46  
47  
48  
49  
50  
51  
52  
53  
54  
55  
56  
57  
58  
59  
60  
61  
62  
63  
64  
65

**Acknowledgements**

Work by GFC was funded by a NERC standard grant (NE/K004328/1). We thank Stuart Kearns for assistance and advice with the Electron Microprobe in Bristol and Chris Ottley and Geoff Nowel for continued help and support in the Durham Geochemistry labs. Richard Arculus, Luca Ziberna, Lena Melekhova, Richard Brooker and Madeleine Humphreys are thanked for many insightful cumulate discussions. Reviews by Etienne Medard, Daniel Smith and editorial handling by Othmar Müntener are greatly appreciated.

## Abstract

1  
2  
3  
4 The Lesser Antilles Volcanic Arc is remarkable for the abundance and variety of erupted  
5  
6 plutonic xenoliths. These samples provide a window into the deeper crust and record a more  
7  
8 protracted crystallisation history than is observed from lavas alone. We present a detailed  
9  
10 petrological and *in-situ* geochemical study of xenoliths from Martinique in order to establish  
11  
12 their petrogenesis, pre-eruptive storage conditions and their contribution to construction of the  
13  
14 sub-volcanic arc crust. The lavas from Martinique are controlled by crystal-liquid  
15  
16 differentiation. Amphibole is rarely present in the erupted lavas but it is a very common  
17  
18 component in plutonic xenoliths, allowing us to directly test the involvement of amphibole in  
19  
20 the petrogenesis of arc magmas. The plutonic xenoliths provide both textural and  
21  
22 geochemical evidence of open system processes and crystal ‘cargos’. All xenoliths are  
23  
24 plagioclase-bearing, with variable proportions of olivine, spinel, clinopyroxene,  
25  
26 orthopyroxene and amphibole, commonly with interstitial melt. In Martinique, the sequence  
27  
28 of crystallisation varies in sample type and differs from other islands of the Lesser Antilles  
29  
30 arc. The compositional offset between plagioclase (~An<sub>90</sub>) and olivine (~Fo<sub>75</sub>), suggests  
31  
32 crystallisation under high water contents and low pressures from an already fractionated  
33  
34 liquid. Texturally, amphibole is either equant (crystallising early in the sequence) or  
35  
36 interstitial (crystallising late). Interstitial amphibole is enriched in Ba and LREE compared  
37  
38 with early-crystallised amphibole and does not follow typical fractionation trends. Modelling  
39  
40 of melt compositions indicates that a water-rich, plagioclase-undersaturated reactive melt or  
41  
42 fluid percolated through a crystal mush, accompanied by the breakdown of clinopyroxene,  
43  
44 and the crystallisation of amphibole. Geothermobarometry estimates and comparisons to  
45  
46 experimental studies imply the majority of xenoliths formed in the mid-crust. Martinique  
47  
48 cumulate xenoliths are inferred to represent crystal mushes within an open system, through  
49  
50 which melt can both percolate and be generated.  
51  
52  
53  
54  
55  
56  
57  
58  
59

## Introduction

60  
61  
62  
63  
64  
65

1  
2 Arc magmas are commonly highly differentiated, and rarely represent primary mantle derived  
3  
4 melts. The vast majority of studies on arc magmatism are restricted to samples of the  
5  
6 extrusive products, which represent the end products of magmatic processes that may occur  
7  
8 over considerable time and depth ranges within the arc crust. On the other hand, plutonic  
9  
10 xenoliths, representing erupted plutonic samples, have a greater preservation potential than  
11  
12 phenocrysts in lavas and are therefore more likely to provide a window into the true  
13  
14 fractionation history of magmas (Arculus and Wills 1980; Macdonald et al. 2000). The Lesser  
15  
16 Antilles Arc is exceptional globally in respect to the abundance and variety of erupted  
17  
18 plutonic xenoliths, which are the focus of several studies (Lewis 1973; Arculus and Wills  
19  
20 1980; Tollan et al. 2012; Stamper et al. 2014). Therefore, the Lesser Antilles is an ideal  
21  
22 location to study the relationship between extrusive and intrusive components of an arc  
23  
24 magmatic system. Our focus is the island of Martinique in the centre of the Lesser Antilles  
25  
26 arc (Fig. 1). We present a detailed petrological, mineralogical and *in-situ* geochemical study  
27  
28 of a diverse collection of plutonic xenoliths from Martinique in order to establish the mode of  
29  
30 formation and the conditions in which they were stored, with the aim of establishing a model  
31  
32 of the components making up the crust and the sub volcanic plumbing system beneath the  
33  
34 island. We use an extensive dataset to address the following key questions: Where in the crust  
35  
36 do the plutonic xenoliths originate from? Do the samples record crystallisation within a  
37  
38 closed system, or do they represent a crystal mush undergoing open system processes? To  
39  
40 what extent do the plutonic xenoliths represent cumulates versus frozen portions of magma?  
41  
42 How does the mineral chemistry vary depending on the evolutionary history? What are the  
43  
44 processes which led to the crystallisation of contrasting amphiboles?  
45  
46  
47  
48  
49  
50

51 There is a vast number of studies focussed on *in-situ* mineral chemistry of volcanic  
52  
53 rocks, however the majority of geochemical and isotopic studies on plutonic rocks have  
54  
55 concentrated on whole rock data. For this study, we focus on the *in-situ* trace element  
56  
57 concentrations of mineral phases contained within a range of plutonic xenolith types. Trace  
58  
59 element variations (in this case, by Laser Ablation ICP-MS) in crystal phases provides a  
60  
61  
62  
63  
64  
65

1 means to track processes throughout the magmatic history of the plutonic xenoliths and the  
2 conditions in which they were formed. By analysing thin sections directly, the textural  
3 relationships of the analysed mineral phases can be assessed, therefore allowing us to  
4 compare the formation processes of different plutonic xenolith types and the nature of  
5 parental melts.  
6  
7  
8  
9

10 The formation and evolution of cumulates and/or crystal mushes has been studied for  
11 layered intrusions such as Skaergaard (McBirney and Noyes 1979; McKenzie 2011) and Rum  
12 (Bédard et al. 1988; Holness 2005; Holness et al. 2007; Leuthold et al. 2014). The generation  
13 of cumulates was traditionally thought to involve crystal settling onto the base of the magma  
14 chamber and then subsequent evolution of the interstitial liquid through crystal growth and  
15 compaction in a closed system (Wager et al. 1960). Solidification likely occurs at magma  
16 chamber margins, therefore exchange of melt to and from the magma chamber may occur.  
17 Crystallisation under these conditions is termed *in-situ* crystallisation (McBirney and Noyes,  
18 1979). However, these models are unlikely to work in hydrous systems such as active island  
19 arcs (Meurer and Claeson 2002). Cumulate rocks from exposed arc crustal sections (Murray  
20 1972; Greene et al. 2006; Bouihol et al. 2015; Stuart et al. 2015) and plutonic xenoliths  
21 (Smith 2014; Stamper et al 2014) can also record evidence for open system processes such as  
22 multiple magma replenishment episodes or percolating melts. Recently, the evolving liquids  
23 interacting with crystal mush and/or cumulate can be traced through the use of *in-situ* trace  
24 element concentrations (Meurer and Claeson, 2002) and large variations in incompatible trace  
25 elements may indicate an open system and an addition of melts into a crystal mush or  
26 cumulate pile. Here we investigate the extent of closed and open system processes recorded  
27 by plutonic xenoliths.  
28  
29  
30  
31  
32  
33  
34  
35  
36  
37  
38  
39  
40  
41  
42  
43  
44  
45  
46  
47  
48  
49  
50

51 Amphibole is rarely present in the erupted volcanic products of the Lesser Antilles  
52 (with the exception of Montserrat), but it is a very common component in plutonic xenoliths  
53 from every island of the Lesser Antilles arc. The trace element signatures of arc lavas suggest  
54 that in a water-rich, mid to lower sub arc crust, the fractionation of amphibole imparts a  
55 control on the differentiation of arc magmas - the amphibole 'sponge' model of Davidson et  
56  
57  
58  
59  
60  
61  
62  
63  
64  
65

1 al. (2007). This model is supported by the presence of ultracalcic nepheline-normative melts  
2 in the lesser Antilles and other island arcs worldwide, which may be generated by the melting  
3 of olivine-clinopyroxene-amphibole cumulates in the lower arc crust (Schiano et al. 2000;  
4 Médard et al. 2004). The plutonic xenoliths from Martinique therefore allow us to directly test  
5 what the involvement of amphibole and ‘cryptic’ amphibole fractionation (Davidson et al.  
6 2007) has on the petrogenesis of erupted arc magmas and the depths in the crust where these  
7 melts are stored and generated. Here, we study amphiboles with contrasting textural  
8 relationships and trace element signatures to explore the different magmatic processes  
9 involved in their formation.  
10  
11  
12  
13  
14  
15  
16  
17  
18  
19  
20  
21

## 22 **Geological Setting**

23  
24  
25

26 The lesser Antilles Arc is located along the eastern margin of the Caribbean plate as the result  
27 of the relatively slow (~2 cm/year) westward subduction of the Atlantic oceanic lithosphere.  
28 The arc is 750 km long and to the north it bifurcates into an older arc to the east and the  
29 recent arc to the west (Fig. 1). The distinct westward jump occurred at ~7 Ma, and has been  
30 attributed to the flattening of the subducting slab by the subduction of an aseismic ridge  
31 (Bouysse and Westercamp 1990). There is an extensive geochemical variation along the arc,  
32 which to a first order is systematic, (Brown et al. 1977; Smith et al. 1980; Turner et al. 1996;  
33 Macdonald et al. 2000), although the large geochemical and isotopic variations at each  
34 volcanic centre add to the complexity (Bezard et al. 2015). In general, islands in the north  
35 (Saba to Montserrat) produce low-K basalts, whereas those to the south (Grenadines and  
36 Grenada) produce medium-K picrites and ankaramites (Macdonald et al. 2000) and only the  
37 southern islands have mafic magmas with >8 wt % MgO and associated mantle-derived  
38 xenoliths (Arculus 1976; Heath et al. 1998). The central islands are typically composed of  
39 medium-K basalt or basaltic-andesite, although many islands have both low- and medium-K  
40 lavas (Macdonald et al. 2000).  
41  
42  
43  
44  
45  
46  
47  
48  
49  
50  
51  
52  
53  
54  
55  
56  
57  
58

59 Seismic refraction experiments (Boynnton et al. 1979) and receiver function analysis  
60  
61  
62  
63  
64  
65

1 (Schlaphorst et al. 2014) reveal a significant variation in the depth of both the inferred  
2 MOHO and Conrad discontinuity along the length of the Lesser Antilles volcanic arc. Similar  
3 along strike crustal variations have been linked to geochemical composition of the erupted  
4 volcanic products, such as in the Izu-Bonin intra-oceanic arc (Kodaira et al. 2007; Tamura et  
5 al. 2009). This implies that the crustal structure imparts a control on the petrogenesis of arc  
6 lavas. In this study, we are able to directly analyse parts of an active plumbing system, at a  
7 potentially diverse range of depths, in order to test the petrogenetic controls of Lesser Antilles  
8 arc crust.  
9

10  
11  
12  
13  
14  
15  
16  
17  
18  
19  
20  
21  
22  
23  
24  
25  
26  
27  
28  
29  
30  
31  
32  
33  
34  
35  
36  
37  
38  
39  
40  
41  
42  
43  
44  
45  
46  
47  
48  
49  
50  
51  
52  
53  
54  
55  
56  
57  
58  
59  
60  
61  
62  
63  
64  
65

Martinique is located in the central arc at the point where the old and current arcs  
diverge and therefore it displays a complete geologic history of the arc, spanning at least the  
last 25 Myr (Germa et al. 2011). Distinct volcanic phases make up the old, intermediate and  
recent volcanic activity in Martinique (Labanieh et al. 2012). The lavas contain, in order of  
abundance, phenocrysts of: plagioclase, orthopyroxene and clinopyroxene. Amphibole is  
typically absent and when present (<5 %) it is opacitized (Davidson and Wilson 2011). The  
lavas from Martinique cover most of the chemical and isotopic variability known in the  
Lesser Antilles arc (Davidson 1983, 1986; Davidson and Wilson 2011). The large range in  
isotopic compositions displayed in Martinique lavas is attributed to the incorporation of slab-  
derived sediment, as well as the addition of sediment melt and fluid via crustal contamination.  
(Davidson and Wilson 2011). The question then arises as to whether the plutonic counterparts  
to the lavas also display the same level of geochemical heterogeneity, or whether the  
processes responsible for the compositional variation occurred in shallow melt dominant  
bodies, unrelated to cumulate crystallisation.

Numerous studies have focused on plutonic xenoliths from the Lesser Antilles  
volcanic arc. Arculus and Wills (1980) provided the first detailed petrological study reporting  
that the compositions of phases within cumulate xenoliths were distinct from the phenocrysts  
in associated eruptives. The majority of xenoliths are ad- and heteradcumulates with fewer  
ortho- and crescumulates. Plagioclase, amphibole, clinopyroxene, orthopyroxene, olivine,  
magnetite, biotite, ilmenite, quartz and apatite are present in various proportions and

1 interstitial glass is often present (Arculus and Wills 1980). Significant variation along the arc  
2 is manifest in the rarity of orthopyroxene and abundance of amphibole in the southern islands,  
3 compared with the common presence of two pyroxenes in the northern islands (Arculus and  
4 Wills 1980). Plutonic xenoliths from each individual island have distinctive characteristics in  
5 terms of mineralogy and petrology (e.g. Arculus and Wills 1980; Kiddle et al., 2010; Stamper  
6 et al., 2014; Tollen et al., 2012) which influences the petrology and geochemistry of the  
7 juvenile erupted material on each of the islands.  
8  
9

### 17 **Analytical Techniques**

20 Whole-rock major (SiO<sub>2</sub>, TiO<sub>2</sub>, Al<sub>2</sub>O<sub>3</sub>, Fe<sub>2</sub>O<sub>3</sub>, MnO, MgO, CaO, Na<sub>2</sub>O, K<sub>2</sub>O, P<sub>2</sub>O<sub>5</sub>) and  
21 selected trace elements (V, Cr, Rb, Nb, Sr, Y, Zn, Co, Ni, Ba) were analysed by X-Ray  
22 Fluorescence spectrometry using a Siemens SRS 3000 sequential XRF spectrometer at the  
23 University of Auckland.  
24  
25

26 Whole-rock trace element analysis was carried out by solution ICP-MS on a  
27 ThermoScientific X-Series 2 ICP-MS at Durham University. W-2, BHVO-1 and AGV-1  
28 standards were used to monitor accuracy and precision (Online Resource 1).  
29  
30

31 Major element concentrations of minerals were analysed *in-situ* on polished thin  
32 sections with Cameca SX100 and JEOL JXA8530F electron microprobes at the University of  
33 Bristol. The Cameca SX100 was run with a 20 kV accelerating voltage, a 20 nA beam current  
34 and a 1 µm spot size. The JEOL JXA8530F was run with a 15 kV accelerating voltage, a 10  
35 nA beam current and a 1 µm spot size. The instruments were calibrated using synthetic oxide,  
36 mineral and metal standards. Typical detection limits are presented in Online Resource 1.  
37  
38

39 Trace element concentrations of minerals were determined by Laser Ablation ICP-  
40 MS using a New Wave UP193FX laser ablation system coupled to a ThermoScientific X-  
41 Series 2 ICP-MS at Durham University. Analyses were made *in-situ* on the same polished  
42 thin sections used for major element analyses. Mineral major element concentrations were  
43 determined for each analytical spot by EPMA prior to LA-ICP-MS analysis. This ensures  
44  
45  
46  
47  
48  
49  
50  
51  
52  
53  
54  
55  
56  
57  
58  
59  
60  
61  
62  
63  
64  
65

1 major and trace element concentrations could be coupled and an accurate  $^{43}\text{Ca}$  (or  $^{29}\text{Si}$ ) value  
2 could be used to normalise LA-ICP MS data. A spot size of 75  $\mu\text{m}$  was used at a laser  
3  
4 repetition rate of 5 Hz and a pulse energy of ~5 mJ. Helium was used as the carrier gas. The  
5  
6 NIST 612 and NIST 610 glasses were used for calibration and to monitor instrumental drift.  
7  
8 BCR-2G and BHVO-2G were used as secondary standards and were analysed during each  
9  
10 analytical session (uncertainties presented in Online Resource 1)  
11  
12  
13  
14

## 15 **Results**

### 20 **Plutonic Xenolith samples**

24 All studied samples are coarse-grained intrusive rocks and are here termed, collectively,  
25  
26 *plutonic xenoliths*. They have been named using the classification scheme of Streckeisen  
27  
28 (1976) and are only termed cumulate if the bulk composition, textures and mineral chemistry  
29  
30 is consistent with them being a subtractive assemblage. If its cumulate origin cannot be  
31  
32 demonstrated through geochemistry, we refer to the rock as a ‘non-cumulate gabbro’, which  
33  
34 in this case, represents a magma that has solidified without significant movement of crystals  
35  
36 with respect to the host melt. The majority of plutonic xenoliths used in this study were  
37  
38 sourced in the north of Martinique, where the most recent phases of volcanism are focussed  
39  
40 (Westercamp 1989; Germa et al. 2011). Most xenoliths were sampled ex situ, from riverbeds  
41  
42 where they have become gravitationally concentrated. Therefore, samples cannot be directly  
43  
44 linked to the deposits in which they were erupted originally. However, the samples used here  
45  
46 are inferred to be from Mount Peleé (126–0 ka) and Mount Conil (550-127 ka) (Westercamp  
47  
48 1989; Germa et al. 2011). The Mount Conil complex is made up of andesitic breccias, lava  
49  
50 domes and lava flows, the majority of which are now buried beneath the younger explosive  
51  
52 deposits of Mount Peleé (Germa et al. 2011), which dominates the north end of the island.  
53  
54  
55  
56

57 The relative crystallisation sequence of each plutonic xenolith can be determined  
58  
59 through textural inspection and this varies between sample types (Fig. 2). Where present,  
60  
61  
62  
63  
64  
65

1 olivine is always the first phase to crystallise, followed by plagioclase which is ubiquitous  
2 and the dominant mineral phase in almost all samples (Fig. 2 and 3). In general,  
3  
4 clinopyroxene is the next phase to crystallise (co-crystallising with orthopyroxene in  
5  
6 gabbronorites). The appearance of spinel varies from the last crystallising phase in olivine  
7  
8 gabbros, after plagioclase in gabbronorites and the first crystallising phase in a hornblende  
9  
10 gabbro sample. In contrast to the lavas, amphibole is an abundant phase, in addition to  
11  
12 clinopyroxene and olivine. Amphibole is either present as an early crystallising phase  
13  
14 alongside plagioclase and clinopyroxene or has crystallised at a late stage and is interstitial to  
15  
16 the cumulus assemblage. Late stage, interstitial amphibole appears to be texturally associated  
17  
18 with clinopyroxene and we explore this relationship below, with *in-situ* trace element  
19  
20 chemistry. Orthopyroxene is present in a number of clinopyroxene bearing samples.  
21  
22  
23

24 Many samples display variations in modal layering, textures and degree of interstitial  
25 melt present. Adcumulate, heteradcumulate and orthocumulate textures are present within  
26  
27 Martinique plutonics and a component of interstitial vesiculated glass is a common feature,  
28  
29 giving rise to a disaggregated appearance (Fig. 3). Where in contact with interstitial glass,  
30  
31 plagioclase may display a lower An rim, representing post-cumulus reaction with the melt.  
32  
33 Melt inclusions are very rare within samples from Martinique. The plutonics can be divided  
34  
35 into the following rock-types: troctolites, olivine-gabbros, hornblende-olivine gabbros,  
36  
37 hornblende gabbros, plagioclase hornblendites, hornblende gabbronorites and gabbronorites.  
38  
39  
40  
41  
42  
43

#### 44 Plutonic types

45  
46 *Troctolites* (ol + plag) are dominated by large plagioclase grains ( $\leq 1$  cm) with smaller ( $\leq 3$   
47  
48 mm [majority  $\ll 1$  mm]) irregular shaped, generally unzoned olivine, which is found both  
49  
50 included within plagioclase and along grain boundaries (Fig. 3a). Interstitial vesiculated  
51  
52 brown glass is present and olivine is normally zoned in respect to Fe-Mg where in contact  
53  
54 with the glass. Plagioclase is unzoned within troctolite samples.  
55  
56  
57

58 *Olivine gabbros* (ol + plag + cpx  $\pm$  spl) have a striking texture dominated by large  
59  
60 poikilitic plagioclase grains ( $\leq 5$  mm) with very small unzoned olivine inclusions ( $< 0.5$  mm)  
61  
62  
63  
64  
65

1 (Fig. 3b). Smaller plagioclase grains (<1 mm) are found interstitially together with poikilitic  
2 clinopyroxene (<10 %, <2 mm) and minor spinel, which contain both plagioclase and olivine.  
3  
4 Plagioclase is unzoned within olivine gabbro samples.  
5

6 *Hornblende-olivine gabbros* (ol + plag + cpx + amph ± opx ± spl) can be subdivided  
7  
8 into two groups based on texture and the appearance of amphibole. One type contains large (3  
9 mm→1 cm) poikilitic amphibole with clinopyroxene inclusions (Fig. 3c). The other type  
10 displays an adcumulate texture (120° grain boundaries) with amphibole appearing  
11 interstitially and in association with clinopyroxene (Fig. 3d). Grains are <3 mm and no  
12 interstitial glass is found in this type. Plagioclase (≤1 cm) is modally dominant (Fig. 2).  
13  
14 Olivine is typically larger (≤3 mm) than in olivine gabbros and often displays weak normal  
15 Fe-Mg zoning. Plagioclase is generally unzoned, apart from one sample in which the  
16 plagioclase has reacted with the host melt, forming a normally zoned rim. Interstitial glass is  
17 present in variable proportions and contains skeletal plagioclase with similar compositions to  
18 the reacted plagioclase rims.  
19  
20  
21  
22  
23  
24  
25  
26  
27  
28  
29  
30

31 *Hornblende gabbros* (plag + cpx + amph ± spl) are characterised by an assemblage  
32 dominated by plagioclase and large (3 mm→1 cm) poikilitic amphibole with both plagioclase  
33 and clinopyroxene inclusions. Clinopyroxene (≤3 mm) also contains inclusions of plagioclase  
34 (Fig. 3e). Plagioclase is unzoned apart from a number of reacted rims where in contact with  
35 interstitial glass.  
36  
37  
38  
39  
40  
41

42 *Plagioclase hornblendites* (plag + amph ± cpx ± spl) are comprised of roughly equal  
43 proportions of large (0.1–1 cm) euhedral amphibole and smaller (<3 mm) plagioclase. An  
44 amphibole grain with a clinopyroxene core is found in one sample and scarce spinel is present  
45 in another. Interstitial glass (>10 %) is characteristic of the plagioclase hornblendite samples  
46 (Fig. 2f). Skeletal plagioclase microlites are found within the vesiculated glass. Plagioclase is  
47 unzoned apart from a number of reacted rims where in contact with interstitial glass.  
48  
49  
50  
51  
52  
53  
54

55 *Hornblende gabbronorites* (plag + amph + cpx + opx ± ol ± spl) are dominated by  
56 plagioclase (normally zoned in a number of samples) and orthopyroxene and clinopyroxene  
57 are present, the former in a greater proportion. Amphibole appears before or together with  
58  
59  
60  
61  
62  
63  
64  
65

1  
2  
3  
4  
5  
6  
7  
8  
9  
10  
11  
12  
13  
14  
15  
16  
17  
18  
19  
20  
21  
22  
23  
24  
25  
26  
27  
28  
29  
30  
31  
32  
33  
34  
35  
36  
37  
38  
39  
40  
41  
42  
43  
44  
45  
46  
47  
48  
49  
50  
51  
52  
53  
54  
55  
56  
57  
58  
59  
60  
61  
62  
63  
64  
65

plagioclase in the crystallisation sequence. Larger amphibole commonly contains inclusions of clinopyroxene and orthopyroxene which may be breaking down (Fig. 3g). Portions of hornblende gabbro samples have a granoblastic texture. Bent plagioclase twins are present in a number of samples indicating some deformation. A number of these samples do not appear to have a cumulate origin.

*Gabbro* (plag + cpx + opx ± spl ± apatite) are dominated by normally zoned plagioclase and are typified by the absence (or trace amounts) of amphibole (Fig. 3h). Both clinopyroxene and orthopyroxene are present, the former in a greater proportion. These samples contain both interstitial magnetite and ilmenite, which crystallised late, and large (1 mm length) needle shaped apatite is also present. Pyroxene exsolution lamellae are present in one non-cumulate gabbro sample. Bent plagioclase twins are present in a number of samples indicating some deformation. These samples do not appear to have a cumulate origin.

### **Lava and plutonic xenolith whole rock chemistry**

Ten crystal-rich lavas and fourteen plutonic xenoliths were analysed for whole rock major and trace element chemistry. The Martinique lavas overlap the compositions of Mt Peleé lavas analysed by Davidson and Wilson (2011). Lavas analysed in this study range from Medium-K basalts to andesites (50–63 wt. % SiO<sub>2</sub>). CaO ranges from 6–11 wt. %, Na<sub>2</sub>O + K<sub>2</sub>O ranges from 3.2–4.8 wt. % and P<sub>2</sub>O<sub>5</sub> from 0.03–0.2 wt. % (Fig. 4). The lavas define typical fractionation trends with decreasing CaO and MgO and increasing total alkalis with increasing SiO<sub>2</sub> (Fig. 4). P<sub>2</sub>O<sub>5</sub> positively trends with SiO<sub>2</sub>, but with some scatter in lavas, and there is no fractionation peak to indicate apatite saturation (Fig. 4). Lavas display typical island arc trace element patterns with enrichment in LILE (Fig. 5a). Chondrite-normalised REE patterns have a concave-up shape, consistent with the removal of amphibole, which is relatively enriched in MREE over HREE (concave-down REE pattern; Fig. 5b). Lava samples display greater enrichments in incompatible elements (Cs, U, Th, Pb, Rb and Ba) than their plutonic counterparts (Fig. 5a).

1 The whole rock chemistry of the plutonic xenoliths is a direct reflection of their  
2 crystal assemblage and the majority of compositions of the analysed samples are consistent  
3 with a cumulate origin. However, three of the analysed gabbroic xenoliths have chemistries  
4 closer to lava compositions and therefore we have termed these *non-cumulate gabbros* (Fig.  
5 4). The plutonic xenoliths lie outside the field defined by the lavas on major element plots and  
6 do not follow a liquid line of descent (Fig. 4). Plutonic xenoliths have higher CaO (>12 wt.  
7 %) and MgO (>5 wt. %) and lower Na<sub>2</sub>O + K<sub>2</sub>O (<3 wt. %) and P<sub>2</sub>O<sub>5</sub> (<0.05 wt. %) to lavas  
8 (Fig. 4). In contrast to lavas, trace element spidergrams reveal plutonic xenoliths have a  
9 stronger positive Sr anomaly, and have positive Ti anomalies (Fig. 5a). Amphibole rich  
10 xenoliths and samples in which amphibole has crystallised early have concave-down  
11 chondrite normalised REE patterns and lack Eu anomalies (Fig. 5b). Xenoliths which are  
12 amphibole free, or in which amphibole has crystallised late, have positive Eu anomalies,  
13 reflecting the high modal proportions of plagioclase (Fig. 2).

14 The amphibole-bearing plutonic xenoliths have higher Dy/Yb ratios (~1.8–2.2) and  
15 lower La (0–7 ppm) than lavas (Dy/Yb ~1.4–1.7, La 6–14 ppm) (Fig. 6). However a subset of  
16 gabbroic (non-cumulate) samples have similar Dy/Yb to lavas (~1.3–1.9). The non-cumulate  
17 gabbros are either hornblende gabbro-norites or gabbro-norites. Minerals from these samples  
18 also have distinctive chemistries (discussed below), suggestive of a different origin to the  
19 cumulate plutonic xenolith samples.

## 20 **Mineral major and trace element chemistry**

21 Here, the *In-situ* major and trace element concentrations of olivine, plagioclase, amphibole,  
22 clinopyroxene, orthopyroxene and spinel are summarised. The range in Mg-number of  
23 olivine, opx, cpx and amphibole, and the An (mol. %) of plagioclase are summarised in  
24 Figure 7. The full dataset is presented in Online Resource 1.

25 Olivine

1 Olivine is present in <50 % of studied samples and has a relatively narrow range in  
2 composition ( $\text{Fo}_{81-68}$ ) (Fig. 8). The olivine is pristine with no signs of alteration to iddingsite  
3 or serpentine, in marked contrast to Grenada (Stamper et al. 2014). CaO contents are <0.25  
4 wt. % and Ni contents are low (40–750 ppm) (Fig. 8). Ni contents are similar to those from  
5 St. Vincent (40–720 ppm; Tollan et al. 2012), but significantly lower than cumulates from  
6 Grenada which range from 0–0.3 wt. % (Stamper et al. 2014). The CaO content varies with  
7 sample type from an average of 0.1 wt. % in hornblende gabbro to 0.2 wt. % in olivine  
8 gabbros (Fig. 8a). The majority of olivine is unzoned; however, where in contact with  
9 interstitial glass, a number of grains display normal zoning (lower Fo rims) reflecting reaction  
10 with interstitial melt. Transition metals are the only group of trace elements with significant  
11 abundances (3200–7600 ppm Mn, 136–390 ppm Zn, 226–336 ppm Co). Mn and Zn  
12 concentrations increase with decreasing Fo but no clear trend is shown by Co.  
13  
14  
15  
16  
17  
18  
19  
20  
21  
22  
23  
24  
25  
26  
27  
28

## 29 Plagioclase

30 Plagioclase is modally dominant in all studied samples (Fig. 2) and is, in general, anorthite-  
31 rich ( $\text{An}_{96-70}$ ; Fig. 7). Those analyses of plagioclase  $<\text{An}_{80}$  are from plagioclase rims, which  
32 are often in contact with interstitial glass, and therefore represent a reacted rim. In the  
33 majority of samples, the interiors of plagioclase are unzoned, apart from in gabbro in  
34 which it is oscillatory zoned. Oscillatory zoned plagioclase are also present within Martinique  
35 lavas (Pichavant et al. 2002; Davidson and Wilson 2011). The range of plagioclase  
36 compositions within the gabbro samples is greater and more sodic ( $\text{An}_{93-51}$ ), and covers  
37 a similar range to zoned plagioclase within Martinique lavas which have calcic cores  $\text{An}_{85-90}$   
38 and sodic rims  $\text{An}_{50-65}$  (Pichavant et al. 2002; Fig. 8b).  
39  
40  
41  
42  
43  
44  
45  
46  
47  
48  
49  
50

51 Plagioclase displays typical REE characteristics of a relative LREE/HREE  
52 enrichment and a positive Eu anomaly. Sr concentrations are higher in an olivine gabbro  
53 sample (900–1300 ppm) compared with a range of 300–550 ppm in other sample types. Sr  
54 and Ba concentrations do not show systematic variations with An. Ba is enriched in  
55 plagioclase from gabbro (11–43 ppm) compared with other sample types (3–20 ppm)  
56  
57  
58  
59  
60  
61  
62  
63  
64  
65

1 (Fig. 8c). Ti (13–154 ppm) and Mn concentrations (18–100 ppm) are highest in olivine  
2 gabbros and lowest within gabbronorites in which spinel has crystallised before plagioclase  
3  
4 (Fig. 8c).  
5  
6  
7

## 8 Clinopyroxene 9

10 Clinopyroxene is present in all samples, with the exception of one troctolite. Compositions  
11 are Ca-, Al- and  $\text{Fe}^{3+}/\Sigma\text{Fe}$  rich diopsides with Mg# 90–67.  $\text{Fe}^{3+}/\Sigma\text{Fe}$ , determined through  
12 stoichiometry, ranges from 0.0–0.6 and decreases with decreasing Mg#. Clinopyroxene from  
13 olivine gabbros and hornblende olivine gabbros the most enriched in  $\text{Fe}^{3+}$ . Gabbronorite  
14 samples have lower Mg compositions (Mg# 77–59) (Fig. 8d). Grains are either unzoned or  
15 have patchy sector zoning. There is a large variation in the concentration of  $\text{Al}_2\text{O}_3$ ;  
16 clinopyroxene from olivine gabbros and hornblende gabbros are enriched (2.5–9.0 wt. %  
17  $\text{Al}_2\text{O}_3$ ) compared with those from gabbronorites (1.0–4.3 wt. %  $\text{Al}_2\text{O}_3$ ). This is reflected in  
18  $\text{Al}^{\text{IV}}$ , with a range in olivine gabbros and hornblende gabbros of  $\text{Al}^{\text{IV}}$  0.1–0.3, compared to  
19  $\text{Al}^{\text{IV}} < 0.1$  in gabbronorites (Fig. 8d).  
20  
21  
22  
23  
24  
25  
26  
27  
28  
29  
30  
31  
32

33 The trace element concentrations of clinopyroxene vary with sample type and  
34 whether amphibole crystallised early or late in the sequence. Clinopyroxene associated with  
35 interstitial amphibole have small  $\text{Eu}/\text{Eu}^* \sim 0.85$  whereas clinopyroxene associated with early  
36 crystallising amphibole does not display an Eu anomaly. Within one olivine gabbro sample  
37 (MQ27), a number of clinopyroxene cores have a strong negative  $\text{Eu}/\text{Eu}^*$  of  $\sim 0.4$  with Mg#  
38 67–82, however the rims of these grains do not have an Eu anomaly and have higher Mg# (80–  
39 90; Fig. 8e).  
40  
41  
42  
43  
44  
45  
46  
47  
48

49 Clinopyroxene displays a large range in incompatible trace elements, highlighted  
50 by the range shown by Hf and Zr (Online Resource 2). Grains from samples containing early  
51 crystallising amphibole have lower concentrations of incompatible trace elements than grains  
52 associated with late crystallising amphibole. The full range in clinopyroxene Hf and Zr from  
53 each type is covered by a single plutonic xenolith sample. All clinopyroxene has enrichments  
54 in MREE and HREE compared to LREE (Fig. 9). In samples with early crystallising  
55  
56  
57  
58  
59  
60  
61  
62  
63  
64  
65

1 amphibole, the clinopyroxene REE patterns have a humped profile compared to a flatter  
2 profile in samples containing late crystallising amphibole (Fig. 9). There is a greater variation  
3  
4 in the LREE concentrations of clinopyroxene associated with late amphibole (La/Yb of 0.17-  
5  
6 1.56) compared to grains in samples in which amphibole crystallised early (La/Yb of 0.13-  
7  
8 0.7).  
9

### 10 11 12 Orthopyroxene

13  
14 Orthopyroxene is present in ~50 % of the studied samples and only occurs in assemblages in  
15  
16 which clinopyroxene is present. Compositions range from Mg# 64–82 (Fig. 7) and En<sub>75–60</sub>  
17  
18 (Online Resource 3) in amphibole bearing cumulate samples. Orthopyroxene in amphibole  
19  
20 free, non-cumulate gabbros are less magnesian (Mg# 64–46 and En<sub>60–44</sub>). Exsolution lamelle  
21  
22 contained in one sample is more calcic (>Wo<sub>4</sub>). Nickel concentrations are lower and Ti  
23  
24 concentrations are higher in olivine bearing gabbros (Ni 10–30 ppm, Ti 840–1670 ppm)  
25  
26 compared with olivine free gabbros (Ni 95–202 ppm, Ti 440–1030 ppm; Online Resource 3).  
27  
28 Zinc (290–400 ppm) and V (45–160 ppm) are consistent between sample types and do not  
29  
30 vary systematically with major element concentrations.  
31  
32  
33  
34  
35  
36  
37

### 38 Amphibole

39  
40 Amphibole compositions based on Leake et al. (2003) vary between sample types; magnesio-  
41  
42 hastingsite are the dominant type in hornblende-olivine gabbros and hornblende gabbros;  
43  
44 tschermakite-pargasite is common in hornblende gabbronorites and magnesio-hornblende in  
45  
46 gabbronorites. Compositions cover a narrow range in regard to Mg# (93–78; Fig. 7), but a  
47  
48 large range in Al (Al<sup>IV</sup> 0.88–2.25) with euhedral, early crystallising amphibole more  
49  
50 aluminium-rich than interstitial and poikilitic amphibole (Fig. 10). Na+K<sup>A</sup> ranges from 0.04–  
51  
52 0.76 and positively correlates (slope=0.51) with Al<sup>IV</sup> indicating temperature sensitive edenite  
53  
54 exchange is significant (Fig. 10a). Ca<sup>B</sup> versus Al<sup>IV</sup> indicates that plagioclase exchange is  
55  
56 significant in amphibole from the majority of plutonic xenoliths (Fig. 10b). However,  
57  
58 plagioclase exchange is insignificant in amphiboles from hornblende gabbronorite samples, in  
59  
60  
61  
62  
63  
64  
65

1 which amphibole crystallised before plagioclase. Al<sup>IV</sup> versus Al<sup>VI</sup> indicates the extent of the  
2 pressure sensitive Al-Tschermack substitution (Fig. 10c). There is no trend in Al<sup>IV</sup> versus Al<sup>VI</sup>  
3 within each xenolith type, with the exception of non-cumulate gabbro. However, differences  
4 in Al<sup>IV</sup> and Al<sup>VI</sup> between xenolith types may suggest a relative shift in crystallisation  
5 pressures.  
6  
7  
8  
9

10  
11 Within Martinique plutonic xenoliths, late stage, interstitial amphibole appears to be  
12 texturally associated with clinopyroxene and this observation is reflected in the trace element  
13 chemistry of amphibole. Like clinopyroxene, amphibole shows a large variation in  
14 incompatible trace elements, highlighted by the range shown by Hf and Zr, which span an  
15 order of magnitude (Online Resource 2). Early amphibole has lower concentrations of  
16 incompatible trace elements (Hf, Zr, Zn) compared with interstitial amphibole, and the ratios  
17 between incompatible trace elements are not consistent across amphibole types (i.e. different  
18 slopes on Hf versus Zr plot [Online Resource 2]). Interstitial amphibole is more enriched and  
19 has a larger range in LREE (and Ba) compared with early amphibole (Fig. 10). This is  
20 particularly evident in amphibole from an olivine gabbro sample (MQ14), which displays a  
21 fivefold variation in La (Fig. 9). Amphibole that has crystallised early displays concave down  
22 or 'humped' REE profile, with a MREE/HREE enrichment and a significant LREE depletion.  
23 In contrast, interstitial amphibole has flatter REE profiles, with less depletion in LREE and  
24 only moderate MREE/HREE fractionation (Fig.12). It is important to note that neither the  
25 early or late crystallising amphibole display a negative Eu anomaly. The amphibole REE  
26 profiles have very similar shape to those of the associated clinopyroxene within sample types  
27 (Fig. 9). This suggests the amphibole may have formed from the breakdown of  
28 clinopyroxene, a reaction that is explored further within the discussion section.  
29  
30  
31  
32  
33  
34  
35  
36  
37  
38  
39  
40  
41  
42  
43  
44  
45  
46  
47  
48  
49  
50

## 51 Spinel

52 Spinel is present in >50 % of studied samples. There are two distinctive spinel compositions  
53 present, depending on the presence of coexisting ilmenite (Online Resource 4). Co-existing  
54 magnetite and ilmenite are present within the three non-cumulate gabbro-norites and these  
55  
56  
57  
58  
59  
60  
61  
62  
63  
64  
65

1 have a higher TiO<sub>2</sub>, lower Al<sub>2</sub>O<sub>3</sub> magnetite present. Within the amphibole bearing cumulate  
2 gabbros, only a single phase, an Al-rich magnetite is present in each sample.  
3  
4  
5

## 6 **Discussion**

### 10 **Mineral chemistry**

11  
12  
13  
14  
15 There is a marked contrast between the composition of plagioclase (high anorthite) and  
16 coexisting (low-Fo) olivine within Martinique plutonic xenoliths, which is a common feature  
17 of plutonic rocks from both the Lesser Antilles and global arc settings (Online Resource 5).  
18 Generally, this is attributed to high H<sub>2</sub>O contents, which suppresses plagioclase crystallization  
19 until the fractionation of mafic phases has substantially depleted the melt in MgO. However,  
20 in plutonic xenoliths from Martinique, plagioclase is a ubiquitous phase and commonly  
21 crystallises before clinopyroxene and amphibole. In addition, the coexisting compositions  
22 have not been reproduced by experimental studies performed on appropriate melt  
23 compositions (Sisson and Grove 1993a; Pichavant and Macdonald 2007). A two-stage  
24 polybaric differentiation could account for the observed plagioclase and olivine compositions,  
25 as suggested for the evolution of St. Vincent magmas (Melekhova et al. 2015). In this case,  
26 the olivine-bearing samples have crystallised from differentiated basaltic andesite magmas,  
27 rather than as residual assemblages from deep crustal source regions, where the melts were  
28 generated (Melekhova et al. 2015). Olivines from Martinique have relatively low Fo and Ni  
29 contents, providing evidence of crystallisation from a melt that has undergone prior olivine  
30 fractionation and is consistent with early differentiation in the deep crust.  
31  
32  
33  
34  
35  
36  
37  
38  
39  
40  
41  
42  
43  
44  
45  
46  
47  
48  
49  
50

51 There is a clear distinction in the major and trace element chemistry of crystal phases  
52 between plutonic xenolith types. It is possible to distinguish whether a sample is of cumulate  
53 origin by using the compositions of crystal phases, and these support the textural evidence  
54 and whole-rock compositions. In general, non-cumulate gabbros contain crystals with a larger  
55 range and more evolved compositions than cumulate equivalents. Non-cumulate gabbros  
56  
57  
58  
59  
60  
61  
62  
63  
64  
65

1 include both gabbro and hornblende gabbro assemblages which represent 'frozen'  
2 portions of a melt. Plagioclase within non-cumulate gabbros are oscillatory zoned and cover a  
3 similar range in compositions to phenocrysts within erupted lavas (Pichavant et al. 2002).  
4 There is a distinctive group of low An and Or (Mol %) plagioclase compositions which lie off  
5 the main trend of the cumulate plagioclase (Fig. 8). This group corresponds to plagioclase  
6 rims within a number of non-cumulate gabbro samples and likely represents crystallisation  
7 after post cumulus interaction with their host lavas. Similarly contrasting chemistries between  
8 cumulate and non-cumulate gabbros are observed in both clinopyroxene and orthopyroxene  
9 (Fig. 8 and Online Resource 3).

### 21 **Intensive variables and the origin of plutonic xenoliths**

22  
23  
24  
25  
26 Determining the storage conditions ( $P$ - $T$ - $H_2O$ - $fO_2$ ) under which Martinique plutonic  
27 xenoliths were formed is essential in understanding the sub-volcanic system beneath  
28 Martinique and the evolution of Martinique eruption products. However, constraining reliable  
29 estimates of Martinique storage conditions remains challenging for the available plutonic  
30 assemblages, and the number of techniques that can be used is limited. Here we use a  
31 combination of geothermometers (Putirka 2016; Ridolfi and Renzulli 2012; Holland and  
32 Blundy 1994; Ghiorso and Evans 2008) and compare the results with the run conditions of  
33 appropriate experimental studies (approach of Stamper et al. 2014). Model and experimental  
34 temperature and pressure estimates for each plutonic xenolith type are shown in Tables 1 and  
35  
36  
37  
38  
39  
40  
41  
42  
43  
44  
45  
46  
47 2.

48  
49 Experimental studies were chosen if their starting compositions fall on the liquid line  
50 of descent, if they reproduce the plutonic types represented in Martinique, and if the phase  
51 compositions are close to that of the natural samples (Online Resource 6; Table 1). If  
52 experimental crystal compositions reproduce those from natural assemblages, the  
53 temperature, pressure and water content can then be inferred from the experimental run  
54 conditions. Experiments by Sisson and Grove (1993a) and Pichavant and MacDonald (2007)

1 suggest shallow olivine gabbro crystallisation (0.1-0.4 GPa) at 1020-1150 °C and high water  
2 contents (saturated and 1.7-5.9 wt. % respectively). Pichavant et al. (2002) experiments  
3 suggest plagioclase hornblendite crystallisation at 0.4 GPa, 945-949 °C and high water  
4 contents (8.2 wt. %). Sisson and Grove (1993a) and Pichavant et al. (2002) experiments  
5 suggest hornblende gabbro crystallisation at 0.2-0.4 GPa, 965-1000 °C and high water  
6 contents (saturated and 6.8 wt. % respectively). We therefore infer a common origin to  
7 plagioclase hornblendite and hornblende gabbro assemblages. Experiments by Pichavant et al.  
8 (2002) and suggest gabbro crystallisation at 0.4 GPa, 950–1016 °C and water contents  
9 from 3.9–6.9 wt. % H<sub>2</sub>O. Experiments by Melekhova et al. (2015) were run at higher  
10 pressures (0.7–1 GPa) and lower water contents (0.6-2.3 wt.%) and the composition of phases  
11 were not as close to natural samples as Pichavant et al. (2002) (Online Resource 6).

24 Model temperature and oxygen fugacity estimates were made using amphibole only  
25 geothermometer of Ridolfi and Renzulli (2012) and Putirka (2016). Within Martinique  
26 xenoliths, interstitial amphibole is not in textural equilibrium with the cumulate phases and  
27 there is no associated interstitial melt available to test for chemical equilibrium. It has also  
28 been shown that H<sub>2</sub>O-rich magmas, which will be relatively Al<sub>2</sub>O<sub>3</sub>-rich will overestimate  
29 crystallisation temperatures (Erdmann et al. 2014). Therefore, amphibole only model  
30 temperatures need to be used with caution. However, the model temperatures in amphibole  
31 bearing samples are within the range of those inferred from experimental studies. Amphiboles  
32 in cumulates using Ridolfi and Renzulli (2012) return model temperatures of 880–1020 °C,  
33 but are lower within non-cumulate gabbros 780–920 °C (Online Resource 7; Fig. 11).  
34 Oxygen fugacity estimates using Ridolfi and Renzulli (2012) are 0.6–3.4  $\Delta$ NNO and vary  
35 between samples (Online Resource 7). Oxygen fugacity estimates of Ghiorso and Evans  
36 (2008) of gabbro samples (both magnetite and ilmenite present) are -0.2–0.8  $\Delta$ NNO.  
37 Model temperatures using the pressure independent model (equation 5) of Putirka (2016)  
38 cover a range of 890–1005 °C in cumulates, and 800–908 °C in non-cumulate gabbros and  
39 are very similar to those of Ridolfi and Renzulli (2012) (Fig. 11). Temperatures were also  
40 calculated using the hornblende-plagioclase model of Holland and Blundy (1994). To  
41  
42  
43  
44  
45  
46  
47  
48  
49  
50  
51  
52  
53  
54  
55  
56  
57  
58  
59  
60  
61  
62  
63  
64  
65

1 increase the likelihood of equilibrium between coexisting hornblende and plagioclase, only  
2 the compositions of crystal rims were used to calculate temperatures. The range in  
3  
4 temperatures from each sample (100–255 °C) is larger than the range of those calculated from  
5  
6 the Ridolfi and Renzulli (2012) and Putirka (2016) models (Online Resource 6; Fig. 11).  
7  
8 Holland and Blundy (1994) model temperatures are also higher, with median values close to  
9  
10 the hottest of Ridolfi and Renzulli (2012) (Fig. 11). The increased range of temperatures is  
11  
12 likely a consequence of disequilibrium between plagioclase and amphibole, particularly in  
13  
14 samples with interstitial (late-stage) amphibole (e.g. samples MQ11 and MQ14; Fig. 11).  
15  
16 Magnetite and ilmenite are only present together within four of the plutonic xenoliths, and  
17  
18 these are classed as non-cumulate gabbros. Where present, temperatures can be estimated  
19  
20 using the Fe-Ti oxide model of Ghiorso and Evans (2008). Model temperatures are lower than  
21  
22 with the other methods (646-909 °C; Fig. 11). This may be a reflection of different storage  
23  
24 conditions and formation of non-cumulate gabbros from more evolved melts.  
25  
26  
27  
28

29         Amphibole compositions have been shown to have a strong pressure dependence (e.g.  
30  
31 Niida and Green 1999; Mandler and Grove 2016). The relative pressure changes between  
32  
33 xenolith types are explored using the pressure sensitive Al-Tschermack substitution, shown  
34  
35 by Al<sup>IV</sup> versus Al<sup>VI</sup> (Fig. 10c). There is no trend in Al<sup>IV</sup> versus Al<sup>VI</sup> within each xenolith type,  
36  
37 with the exception of non-cumulate gabbro, indicating limited pressure control. This is  
38  
39 particularly evident in hornblende gabbronorites, where Al<sup>VI</sup> shows a large range with  
40  
41 little/no corresponding change in Al<sup>IV</sup> and therefore are likely to be controlled by variations in  
42  
43 melt chemistry. However, differences in Al<sup>IV</sup> and Al<sup>VI</sup> between xenolith types suggest a  
44  
45 relative shift in crystallisation pressures between non-cumulate gabbro and hornblende  
46  
47 gabbronorite at lower pressures, and hornblende gabbro, hornblende olivine gabbro and  
48  
49 plagioclase hornblendite at higher pressures (Fig. 10c). Pressure estimates using the  
50  
51 amphibole only barometers of Putirka (2016), Ridolfi et al. (2010) and Ridolfi and Renzulli  
52  
53 (2012) have been shown to have very large uncertainties (Erdmann et al. 2014; Putirka 2016),  
54  
55 and were therefore not calculated for this study.  
56  
57  
58  
59

60         The comparison to experimental studies suggests that all Martinique assemblages can  
61  
62  
63  
64  
65

1  
2  
3  
4  
5  
6  
7  
8  
9  
10  
11  
12  
13  
14  
15  
16  
17  
18  
19  
20  
21  
22  
23  
24  
25  
26  
27  
28  
29  
30  
31  
32  
33  
34  
35  
36  
37  
38  
39  
40  
41  
42  
43  
44  
45  
46  
47  
48  
49  
50  
51  
52  
53  
54  
55  
56  
57  
58  
59  
60  
61  
62  
63  
64  
65

be produced under high water contents and pressures  $\leq 0.4$  GPa corresponding to depths of  $\leq 15$  km. Therefore, all plutonic xenoliths from Martinique are samples from mid-upper crustal storage regions and high water contents play an important role in the petrogenesis of magmas. The high anorthite content in plagioclase, high wollastonite content in clinopyroxene, and amphibole compositions indicate crystallisation from a hydrous magma (Gaetani et al. 1993; Sisson and Grove 1993a; Claeson and Meuer 2004). The presence of amphibole within Martinique plutonic xenoliths suggests that mid-upper crystal mushes can act as a sponge, storing and supplying the final erupted melts with water. Davidson and Wilson (2011) apply the geohygrometer of Pichavant and Macdonald (2007) to Martinique lavas, which gives water contents of 3.1–4.5 wt. % H<sub>2</sub>O (assuming a temperature of crystallisation of 1050°C). Such H<sub>2</sub>O contents are consistent with extensive amphibole crystallization in deep crustal magma reservoirs (Davidson and Wilson 2011), such as the storage regions we directly analyse in this study.

No plagioclase-free assemblages were sampled from Martinique and there is no evidence that any Martinique plutonic xenoliths have an origin in the lower crust. In hydrous conditions at greater pressures and depths, plagioclase is likely to be absent (Melekhova et al. 2015). Plagioclase-free assemblages have been sampled on Grenada (Stamper et al. 2014) and St. Vincent (Tollan et al. 2012) to the south of the Lesser Antilles arc and plagioclase appears later in the crystallisation sequence in plutonic xenoliths from Grenada. These distinctions may reflect a different crustal structure beneath the islands (Boynton et al. 1979), coupled with a contrasting polybaric petrogenesis.

### **Amphibole and reactive melt flow**

In contrast to Grenada (Stamper et al. 2014), plutonic xenoliths from Martinique do not have a consistent crystallisation sequence. This is particularly evident in the early or late appearance of amphibole, which are both texturally and compositionally distinct. A variable crystallisation sequence may suggest that the plutonic xenoliths from Martinique are formed

1 from more than one parental melt with distinct evolutionary history and H<sub>2</sub>O content, or they  
2 represent the same melt at a different stage of evolution. Amphibole trace element chemistry,  
3  
4 together with textural evidence, provide evidence that multiple melts were involved in the  
5  
6 petrogenesis of Martinique plutonic xenoliths. Early crystallising (equant) amphibole is more  
7  
8 aluminium rich (both Al<sup>IV</sup> and Al<sup>VI</sup>), and has lower concentrations of incompatible trace  
9  
10 elements (Online Resource 2), LREE and Ba than late (interstitial and poikilitic) amphibole  
11  
12 (Fig. 10). Melt SiO<sub>2</sub> (wt. %) in equilibrium with early and interstitial amphibole was  
13  
14 estimated using formulations from Putirka (2016). Early amphibole returned melts with 50.3–  
15  
16 52.8 wt. % SiO<sub>2</sub> compared with more evolved compositions of 58.8–64.6 wt. % SiO<sub>2</sub> from  
17  
18 interstitial amphibole (online Resource 7). Predicted melt compositions of ~70 wt. % SiO<sub>2</sub>,  
19  
20 and the similarity of mineral chemistry from non-cumulate gabbros and lavas suggests that  
21  
22 the non-cumulate gabbros are associated with the final erupted magmas.  
23  
24  
25

26  
27 The question then arises as to whether the late-stage amphibole crystallised in a  
28  
29 closed system from the residual melt after crystallisation of the other phases (e.g. McBirney  
30  
31 and Noyes 1979; Morse 1996), or in an open system involving the input of percolating  
32  
33 reactive melts or liquids (Reiners 1998; Coogan et al. 2000, 2001; Meurer and Claeson 2002;  
34  
35 Leuthold et al. 2014; Smith 2014; Bouihol et al. 2015; Stuart et al. 2016). It has been shown  
36  
37 that the products of reactive liquid flow will differ from one produced by simple  
38  
39 crystallisation along a liquid line of descent (Reiners 1998) and the addition of low degree  
40  
41 melts cause large variations in incompatible trace elements. In Martinique samples, there is an  
42  
43 order of magnitude variation in incompatible elements (Hf and Zr) in amphibole and  
44  
45 clinopyroxene (Online Resource 2) and a 5-fold variation in La of amphibole is observed  
46  
47 within one sample (Fig. 9). Trace element concentrations of interstitial amphibole do not  
48  
49 follow the trend predicted if fractional crystallisation controlled the melt chemistry during  
50  
51 amphibole crystallisation (Fig. 10d). This suggests that there has been some addition of melt  
52  
53 into the system. This evidence is supported by the lack of a negative Eu anomaly in interstitial  
54  
55 amphibole. If interstitial amphibole crystallised from a residual melt after significant  
56  
57 plagioclase crystallisation, then the amphibole should have a negative Eu anomaly. This  
58  
59  
60  
61  
62  
63  
64  
65

1 implies that the invading melt was yet to undergo plagioclase saturation, or that the melt was  
2 more water-rich and oxidising, leading to the suppression of the Eu anomaly in high An  
3 plagioclase (Philpotts 1970; Deering and Bachmann 2010).  
4  
5

6 Amphibole partition coefficients from calc-alkaline fractional crystallisation  
7 experiments of Nandedkar et al. (2016) were used to estimate melts in equilibrium with early,  
8 late and non-cumulate amphibole (Fig. 12a). Partition coefficients from a basaltic andesite  
9 (RN8 Inner), run at 1010 °C and a dacite (RN13V2) at 860 °C were chosen (Fig. 12a). Melt  
10 estimates using both experiments have the same REE profile shapes, however higher melt  
11 REE concentrations are predicted using partition coefficients of the basaltic-andesite sample.  
12  
13 Melts predicted using the late, interstitial amphibole has similar MREE-HREE pattern as the  
14 erupted lavas, but is significantly more enriched in LREE. In contrast, early crystallised  
15 amphibole returns melts with a flatter profile. The offset between REE concentrations  
16 predicted using the two experiments (RN8 Inner and RN13V2) highlights the extent to which  
17 amphibole partition coefficients vary with melt fractionation. Melts predicted using the  
18 partition coefficients from Sisson (1994) and Adam and Green (2003) have the same relative  
19 trends as those from Nandedkar et al. (2016) and suggest early amphibole grains crystallised  
20 from a primitive melt with a flat REE profile. The late, interstitial amphibole was crystallised  
21 from a melt enriched in LREE, similar to both the erupted lava whole-rock compositions and  
22 the melt in equilibrium with amphiboles in non-cumulate gabbros (Fig. 12b). This suggests  
23 that interstitial amphibole crystallised from evolved melts (58.8–64.6 wt. % SiO<sub>2</sub>) which  
24 either infiltrated into a pre-existing cumulate pile (or mush), or the erupted melts were  
25 themselves generated in, and extracted from the crystal mush.  
26  
27  
28  
29  
30  
31  
32  
33  
34  
35  
36  
37  
38  
39  
40  
41  
42  
43  
44  
45  
46  
47  
48

49 Clinopyroxene partition coefficients from Adam and Green (2003) and Wood and  
50 Blundy (1997) reveal the melts in equilibrium with clinopyroxene associated with both  
51 amphibole types have similarly contrasting REE compositions. The shape of the REE profile  
52 for melt in equilibrium with clinopyroxene associated with interstitial amphibole is very  
53 similar to the melt in equilibrium with interstitial amphibole. This suggests that a peritectic  
54 reaction occurred, in which clinopyroxene reacted with the infiltrating melt and was replaced  
55  
56  
57  
58  
59  
60  
61  
62  
63  
64  
65

1 by the interstitial amphibole. This geochemical evidence is in agreement with the textural  
2 observations (Fig. 3). However, the estimated REE concentrations are lower than both the  
3  
4 erupted lavas and the melt in equilibrium with interstitial amphibole (Fig. 12). This  
5  
6 observation implies that an addition of trace elements, in particular LREE into the system  
7  
8 must have occurred after clinopyroxene crystallisation and before amphibole crystallisation.  
9  
10 To assess the contribution of elements (Li, Al, Ti, Ga, Rb, Sr, Y, Zr, Hf, Nb, Ta, Ba, La, Ce,  
11  
12 Sm, Ho, Yb, Lu, Th, U) from clinopyroxene to produce reaction replacement amphiboles, the  
13  
14 melt produced from the breakdown of clinopyroxene was modelled using partition  
15  
16 coefficients (run at 1025 °C, 0.5 GPa) from Adam and Green (2003) (Fig. 13). The chemistry  
17  
18 of amphibole which then crystallised from the clinopyroxene melt was modelled using  
19  
20 experimental amphibole partition coefficients (run at 1000 °C, 0.5 GPa) from Adam and  
21  
22 Green (2003). If the modelled amphibole element concentrations were lower than natural  
23  
24 interstitial amphibole, then an additional source of elements is needed (Fig. 13). The modal  
25  
26 proportions of clinopyroxene and reaction replacement amphibole (e.g. MQ14; Fig. 2)  
27  
28 suggest a significant proportion of clinopyroxene has been replaced by amphibole. Melting of  
29  
30 up to 20% clinopyroxene can supply the system with the concentrations of Al, Ti and the  
31  
32 majority of trace elements needed to reproduce interstitial amphibole compositions. Apart  
33  
34 from low degrees of melting (1% cpx melting), a minimum additional source of Sr, Ba, Y and  
35  
36 Zr, as well as H<sub>2</sub>O and Na are needed in order to produce the interstitial amphibole (Fig. 13).  
37  
38 Therefore, a water-rich plagioclase-undersaturated melt, carrying fluid-mobile elements,  
39  
40 reacted with the cumulate/mush pile to produce late-stage interstitial amphibole. The reaction  
41  
42 of clinopyroxene with a melt, to form amphibole has been observed in cumulates (Best 1975;  
43  
44 Debari et al. 1987; Coogan et al. 2001; Smith 2014; Bouihol et al. 2015) and we believe this  
45  
46 is a common process in Martinique plutonic xenoliths.  
47  
48  
49  
50  
51  
52  
53  
54  
55

### 56 **Open system processes**

57  
58  
59

60 In addition to the percolating melts discussed above, plutonic xenoliths from  
61  
62  
63  
64  
65

1  
2  
3  
4  
5  
6  
7  
8  
9  
10  
11  
12  
13  
14  
15  
16  
17  
18  
19  
20  
21  
22  
23  
24  
25  
26  
27  
28  
29  
30  
31  
32  
33  
34  
35  
36  
37  
38  
39  
40  
41  
42  
43  
44  
45  
46  
47  
48  
49  
50  
51  
52  
53  
54  
55  
56  
57  
58  
59  
60  
61  
62  
63  
64  
65

Martinique display additional textural and chemical evidence of open system behaviour in the form of crystal cargos. One olivine gabbro sample (MQ27) shows clear evidence for the assembly of crystal cargos. Clinopyroxene cores within this sample have a larger negative  $\text{Eu}/\text{Eu}^*$  of  $\sim 0.4$  and a lower  $\text{Mg}\#$  than the rims, which do not have an Eu anomaly and have a higher  $\text{Mg}\#$  (Fig.8). This may suggest that the clinopyroxene grains began growing from a melt that had undergone significant plagioclase crystallisation, and then interacted with and continued to grow in a lesser-evolved, plagioclase undersaturated melt. Alternatively, the rim forming melt may be more water-rich and oxidising, leading to the suppression of the Eu anomaly in high An plagioclase (Philpotts 1970; Deering and Bachmann 2010). Oxygen fugacity estimates from sample MQ27 amphiboles are particularly oxidising (2.2-2.9  $\Delta\text{NNO}$ ; Ridolfi and Renzulli 2012) and may therefore account for the absence of a negative Eu anomaly in clinopyroxene. This evidence suggests that the plutonic xenoliths from Martinique represent the assembly of grains during transport and emplacement, and are not formed through closed system crystallisation after emplacement of a magma body. The plagioclase undersaturated melt is consistent with the estimated composition of the percolating reactive melt described above.

The xenoliths commonly contain vesiculated interstitial glass, and few samples have a locked crystal framework. This textural evidence suggests the plutonic xenoliths are capturing the disaggregation of a crystal mush (Passmore et al., 2012). This may represent interaction at the margins of magma reservoirs stored within a larger scale mush zone. In a number of samples, edges of crystals (plagioclase and olivine) in contact with the interstitial melt have a distinctive normally zoned reaction rim of more evolved compositions. This suggests that it was an evolved melt which infiltrated a cumulate pile or mush and ‘post-cumulus’ growth of the crystals occurred prior to eruption. Within a number of samples, cross veins of recrystallised material are present. In this case the infiltration of melt was confined to veins and did not disrupt the original crystal framework. The interstitial glass (Fig. 3a, f) contains skeletal plagioclase microlites, suggesting the host melt was rapidly quenched and therefore the infiltration of the host melt must have occurred in a short timescale prior to

1 eruption. Reacted rims on plagioclase are close to the compositions of plagioclase in non-  
2 cumulate gabbros (Fig. 8), and those from lavas (Pichavant et al. 2002). This provides  
3  
4 evidence that the crystal mush interacted with the final erupted melts, that are associated with  
5  
6 non-cumulate gabbros.  
7

8  
9 Melt migration through crystal mushes is a common process within crustal storage  
10 regions (Leuthold et al. 2014; Solano et al. 2014). Exposed roots of volcanic arcs, such as the  
11 Kohistan palaeo-island arc, Pakistan (Bouihol et al. 2015), Talkeetna, Alaska (Greene et al.  
12 2006), Fjordland, New Zealand (Stewart et al. 2016) and exposed ultramafic complexes,  
13  
14 Alaska (Murray 1972; Irvine 1974) allow for direct observations of the lower crust, and  
15  
16 provide an analogue to Martinique plutonic xenoliths. In Kohistan, kilometre scale magmatic  
17  
18 conduits are present in the lower crust, which melt rose through and reacted with the existing  
19  
20 cumulate assemblages (Bouihol et al. 2015). These conduits are similar to crustal feeder pipes  
21  
22 observed in ultramafic complexes, Alaska (Murray 1972; Irvine 1974). Within these crustal  
23  
24 sections there are outcrop scale variations in cumulate textures and crystallising phases,  
25  
26 suggesting that it is possible to source variable plutonic xenoliths from relatively localised  
27  
28 zones. The evidence of infiltrating melts and open system processes within Martinique  
29  
30 cumulates suggest that they may be sourced from similar melt-rich zones, which feed shallow  
31  
32 storage regions within the Lesser Antilles crust.  
33  
34  
35  
36  
37  
38  
39  
40  
41

### 42 **Amphibole sponge model**

43  
44  
45

46 Amphibole accumulation, represented by amphibole bearing plutonic xenoliths can be seen to  
47  
48 have a control on the trace element signature of the lavas (Fig. 5). Amphibole preferentially  
49  
50 incorporates MREE over HREE and therefore fractionation of amphibole will drive the melt  
51  
52 to lower MREE/HREE (e.g. Dy/Yb) with an increasing concentration of an incompatible  
53  
54 element (e.g. La). The fractionation of the final erupted amphibole-free lava assemblage does  
55  
56 not have any leverage on the Dy/Yb ratio, therefore fractionation of the cumulate assemblage  
57  
58 can explain the variation in Dy/Yb displayed by the lavas (Fig. 6). The non-cumulate gabbro  
59  
60  
61  
62  
63  
64  
65

1 samples can be produced from the fractional crystallisation of the evolved melts generated  
2 after the initial 'cryptic' amphibole fractionation and we therefore infer these samples to  
3  
4 relate to crystallisation associated with the final erupted melt-dominant bodies stored in the  
5  
6 shallow crust.  
7

8  
9 The data presented in this study suggests that a percolating melt through a crystal  
10  
11 mush, aided the breakdown of clinopyroxene and growth of amphibole (Best 1975; Debari et  
12  
13 al. 1987; Smith 2014). The reactive transport of a melt through a clinopyroxene mush to  
14  
15 crystallise amphibole will impart an amphibole fractionation signature irrespective of  
16  
17 amphibole appearance or absence as a phenocryst phase (Smith 2014). Therefore, the  
18  
19 presence of precursory clinopyroxene is a key requirement for the amphibole sponge in the  
20  
21 mid-lower Lesser Antilles arc crust. The growth of interstitial amphibole as a replacement to  
22  
23 clinopyroxene allows more interstitial liquid to be incorporated in the cumulates than would  
24  
25 be possible in dryer basaltic systems with only amphibole-free assemblages (Meurer and  
26  
27 Claeson 2002). Therefore, the mid-crustal storage regions provide a fertile source for melts  
28  
29 and fluids to fuel eruptions and potentially increase the explosivity of the magmas that reach  
30  
31 the surface.  
32  
33  
34  
35  
36  
37

### 38 **Plumbing system beneath Martinique**

39  
40  
41

42 The plutonic xenoliths from Martinique used in this study provide direct evidence of open  
43  
44 system processes and the majority were sourced from the mid-crust and represent regions of  
45  
46 crystal mush, within which melts are both stored and generated. Melt segregation in hot zones  
47  
48 (Sawyer 1994; Solano et al. 2012, 2014) provides mechanisms by which a largely crystal-free  
49  
50 melt is separated from the early-formed clinopyroxene and reaction replacement amphibole  
51  
52 rich mushes. We can infer that the lower crust was likely a deep crustal hot zone (Annen et al.  
53  
54 2006). Melts were generated and stored within this region and underwent early differentiation  
55  
56 of olivine (plus other phases) from mantle-derived primitive melts. The relatively low Fo and  
57  
58 Ni contents of olivine provide evidence of crystallisation from a melt that has undergone prior  
59  
60  
61  
62  
63  
64  
65

1  
2  
3  
4  
5  
6  
7  
8  
9  
10  
11  
12  
13  
14  
15  
16  
17  
18  
19  
20  
21  
22  
23  
24  
25  
26  
27  
28  
29  
30  
31  
32  
33  
34  
35  
36  
37  
38  
39  
40  
41  
42  
43  
44  
45  
46  
47  
48  
49  
50  
51  
52  
53  
54  
55  
56  
57  
58  
59  
60  
61  
62  
63  
64  
65

olivine fractionation. Melts that segregate from the deep crustal hot zone ascend and stall in the mid crust, within the plagioclase stability field. The vast majority of cumulate xenoliths from Martinique represent storage within this mid-crustal mush zone. Variations in phase assemblages may relate to localised variations in water content and temperatures within the crystal mush. Hydrous reactive melts percolate through the cumulate pile, crystallising interstitial amphibole. A large proportion of the plutonic xenoliths contain evidence for percolative melt flow and therefore likely originated in melt rich channels within a crystal mush (Bouihol et al. 2015). For this reason, the erupted plutonic record may be biased to sampling melt rich zones which can eventually transport parts of the cumulate pile into the host magmas in shallow reservoirs. Crystal poor, evolved melts generated within the mid-crustal mush zone segregate and ascend to their pre-eruptive storage in shallow magma reservoirs for some time prior to eruption. The non-cumulate gabbros generally have zoned crystal phases with more evolved compositions, some amphibole-free assemblages and whole-rock chemistries which resemble erupted lavas, and therefore appear to represent the plutonic equivalents of the final erupted melts, or frozen portions of magma chambers. The ability of amphibole-rich cumulates in the mid-crust to act as a sponge provides a source for water rich magmas, which may eventually fuel the explosive eruptions characteristic of the Lesser Antilles volcanic arc.

## 42 **Conclusions**

43  
44  
45  
46  
47  
48  
49  
50  
51  
52  
53  
54  
55  
56  
57  
58  
59  
60  
61  
62  
63  
64  
65

Plutonic xenoliths from Martinique provide direct evidence for the amphibole sponge model in arc crust and the nature of the sub-volcanic plumbing system. The key findings from Martinique plutonic xenoliths are the following:

1. Crystallisation sequences of the plutonic xenoliths are variable, which could be accounted for by multiple sources of melt that differentiated at multiple depths. This observation is in contrast to plutonic xenoliths from other islands of the Lesser Antilles which have consistent crystallisation sequences.

- 1  
2  
3  
4  
5  
6  
7  
8  
9  
10  
11  
12  
13  
14  
15  
16  
17  
18  
19  
20  
21  
22  
23  
24  
25  
26  
27  
28  
29  
30  
31  
32
2. All samples are inferred to be sourced from the mid-upper crust  $\leq 15$  km, at pressures of  $\leq 4$  GPa and crystallised under high water contents. Plutonic xenoliths of cumulate origin represent a mid-crustal storage region, whereas non-cumulate gabbros and gabbro-norites are associated with melt dominant bodies stored in the upper crust.
  3. There is clear textural and geochemical evidence for open system processes including crystal cargos and percolating reactive melts. Therefore plutonic xenoliths from Martinique represent mid-crustal crystal mushes in which melts can be both stored and generated.
  4. Precursory clinopyroxene is a key requirement of amphibole sponge in the Lesser Antilles arc crust. Percolating melts, react with clinopyroxene to form interstitial amphibole. This is seen both texturally and in trace element concentrations of associated clinopyroxene and amphibole, where the chemistries of precursory clinopyroxene, together with an evolved percolating melt, control the composition of the later crystallised amphibole.

### 33 **Figure Captions**

34  
35  
36  
37

38 **Fig. 1.** Map of the Lesser Antilles Island arc. The dashed line depicts the approximate  
39 position of the subduction zone (after Wadge and Shepherd 1984). Islands making up the old  
40 arc (brown) and the currently active arc (green) are denoted.  
41  
42

43 **Fig. 2.** Modal proportions of crystal phases within Martinique plutonic xenoliths (excluding  
44 vesiculated glass). Mineral modes were obtained through point counting of thin sections.  
45  
46 Samples are listed from top to bottom by decreasing Fo of olivine followed by An of  
47 plagioclase. Names are based on the classification scheme of Streckeisen (1976). The  
48 crystallisation sequence (based on textural inspection) of each sample is also given.  
49  
50  
51  
52  
53

54 **Fig. 3.** Photomicrographs of plutonic xenolith types displaying characteristic textures. (a)  
55 Troctolite with large plagioclase and smaller olivine. Olivine in contact with interstitial glass  
56 is zoned. (b) Olivine gabbro with distinctive texture with large plagioclase grains with many  
57  
58  
59  
60  
61  
62  
63  
64  
65

1 small inclusions of olivine. (c) Hornblende-olivine gabbro displaying poikilitic amphibole  
2 with clinopyroxene inclusions. (d) Hornblende-olivine gabbro with interstitial amphibole  
3 surrounding clinopyroxene. (e) Hornblende gabbro with plagioclase included in  
4 clinopyroxene and amphibole. (f) Plagioclase hornblendite with characteristic interstitial  
5 glass. (g) Hornblende gabbro with poikilitic amphibole with clinopyroxene and  
6 orthopyroxene inclusions. (h) Gabbro with 120° equilibrium grain boundaries. Both (g)  
7 and (h) are termed non-cumulate gabbros (see text).

8  
9  
10  
11  
12  
13  
14  
15 **Fig. 4.** Whole-rock major element chemistry of Martinique cumulates and lavas from this  
16 study and Davidson and Wilson (2011).

17  
18  
19  
20 **Fig. 5.** (a) Extended whole-rock trace element spidergram and (b) REE diagram of  
21 Martinique lavas (data from Davidson and Wilson (2011) and this study) and plutonic  
22 xenoliths, normalised to primitive mantle (Palme and O'Neill 2003).

23  
24  
25  
26  
27 **Fig. 6.** Whole-rock La versus Dy/Yb of Martinique lavas and plutonic xenoliths. Solid and  
28 dashed lines are modelled melt vectors from the fractional crystallisation of either the lava  
29 phenocryst or the cumulate assemblage (after Davidson and Wilson 2011).

30  
31  
32  
33 **Fig. 7.** Summary of phase compositions for the range of studied plutonic xenolith types: Mg#  
34 (100 Mg/(Mg+Fe<sup>2+</sup>)) of olivine, orthopyroxene, clinopyroxene, amphibole, and An (mol %) of  
35 plagioclase. Samples are ordered based on the mean clinopyroxene Mg#.

36  
37  
38  
39  
40 **Fig. 8.** (a) Olivine Fo versus CaO (wt. %) from different plutonic xenolith types. Grey shaded  
41 area in represents range covered by Grenada cumulates (Stamper et al. 2014). (b) Major and  
42 (c) trace element chemistry of plagioclase from different plutonic xenolith types. Grey shaded  
43 areas represent the compositional range covered by plutonic xenoliths with a cumulate origin.  
44 (d) Major element variations of clinopyroxene from different plutonic xenolith types. (e) Mg#  
45 versus Eu/Eu\* of clinopyroxene from samples with either early or interstitial amphibole.

46  
47  
48  
49  
50  
51  
52  
53 **Fig. 9.** REE patterns of amphibole and clinopyroxene types normalised to primitive mantle  
54 values (Palme and O'Neill 2003). Black lines within the shaded area of late stage, interstitial  
55 amphibole are the REE in one sample to show the variation in LREE.

56  
57  
58  
59  
60 **Fig. 10.** Major and trace element variations of amphibole. Structural components (Leake et al.

1  
2  
3  
4  
5  
6  
7  
8  
9  
10  
11  
12  
13  
14  
15  
16  
17  
18  
19  
20  
21  
22  
23  
24  
25  
26  
27  
28  
29  
30  
31  
32  
33  
34  
35  
36  
37  
38  
39  
40  
41  
42  
43  
44  
45  
46  
47  
48  
49  
50  
51  
52  
53  
54  
55  
56  
57  
58  
59  
60  
61  
62  
63  
64  
65

1997) are used to show variation in major elements and (a) edenite, (b) plagioclase and (c) Al-Tschermak exchange. The trace element variations of early, interstitial and non-cumulate gabbro amphibole (d-f) highlight enrichments in LREE and fluid mobile elements within interstitial amphibole.

**Fig. 11.** Comparison of temperature estimates using the hornblende-plagioclase model of Holland and Blundy (1994). and the amphibole only models of Ridolfi and Renzulli (2012) and Putirka (2016). In non-cumulate gabbro samples, which contained co-existing magnetite and ilmenite, the Fe-Ti oxide model of Ghiorso and Evans (2008) was used.

**Fig. 12.** Modeled melt compositions, normalised to primitive mantle (Palme and O'Neill 2003) in equilibrium with amphibole (a & b) and clinopyroxene (c) types using REE partition coefficients (Sisson 1994; Wood and Blundy 1997; Adam and Green 2003; Nandedkar et al. 2016). Grey shaded area is the range in whole-rock REE of erupted Martinique lavas.

**Fig. 13.** (a) Modeled trace element concentrations of the liquid produced through varying degrees of clinopyroxene melting (coloured lines). The compositions of clinopyroxene (grey line) and associated interstitial amphibole (black line) are shown for comparison. (b) The difference in concentration between interstitial amphibole and the liquid produced from clinopyroxene melt. Strong positive values indicate those elements that were added through an additional source such as a percolating melt.

### Online Resource Captions

**Online Resource 1.** Excel file of Supplementary Data.

**Online Resource 2.** Zr versus Hf of amphibole and clinopyroxene from samples with either early or late crystallising amphibole, and amphiboles from non-cumulate gabbros. A large variation (nearly an order of magnitude) in incompatible trace elements is shown.

**Online Resource 3.** (a) En versus Wo of orthopyroxene from different plutonic xenolith types. (b) Ti versus Ni of orthopyroxene from olivine bearing cumulates and non-cumulate

gabbros.

**Online Resource 4.** Mg # versus Al<sub>2</sub>O<sub>3</sub> and TiO<sub>2</sub> of spinel from cumulates and non-cumulate gabbros.

**Online Resource 5.** Coexisting plagioclase (Mol % An) and olivine (Mol % Fo) from plutonic xenoliths from Martinique and other islands of the Lesser Antilles. Compositions from the Lesser Antilles cover a similar range to those from other arcs worldwide (Sisson and Grove 1993b). Arrow marks a core to rim change in plagioclase An within one Martinique sample.

**Online Resource 6.** Comparisons of mineral compositions in experimental troctolites, olivine gabbros, plagioclase hornblendites, hornblende gabbros, gabbronorites and hornblende gabbronorites with compositions from natural plutonic xenolith samples. Experimental run conditions from the different studies are shown. Grey shaded areas indicates the range of natural compositions in plutonic xenoliths from Grenada (Stamper et al. 2014).

**Online Resource 7.** Model estimates of temperature, oxygen fugacity and melt SiO<sub>2</sub> composition for Martinique plutonic xenoliths.

## References

- Adam J, Green TH (2003) The influence of pressure, mineral composition and water on trace element partitioning between clinopyroxene, amphibole and basanitic melts. *European Journal of Mineralogy* 15:831-841
- Annen C, Blundy JD, Sparks RSJ (2006) The genesis of intermediate and silicic magmas in deep crustal hot zones. *Journal of Petrology* 47(3):505-539
- Arculus R (1976) Geology and geochemistry of the alkali basalt-andesite association of Grenada, Lesser Antilles island arc. *Geological Society of America Bulletin* 87(4):612-624

1 Arculus RJ, Wills KJA (1980) The petrology of plutonic blocks and inclusions from the  
2 Lesser Antilles Island Arc. *Journal of Petrology* 21(4):743-799  
3

4  
5 Bédard JH, Sparks RSJ, Renner R, Cheadle MJ, Hallworth MA (1988) Peridotite sills and  
6 metasomatic gabbros in the eastern layered series of the Rum complex. *Journal of the*  
7  
8  
9  
10 *Geological Society* 145:207-224 doi:10.1144/gsjgs.145.2.0207  
11

12  
13 Best MG (1975) Amphibole-bearing cumulate inclusions, Grand Canyon, Arizona and their  
14 bearing on silica-undersaturated hydrous magmas in the upper mantle. *Journal of Petrology*  
15  
16  
17  
18 16(1):212-236  
19

20  
21 Bezard R, Turner S, Davidson JP, Macpherson CG, Lindsay JM (2015) Seeing through the  
22 effects of crustal assimilation to access the source composition beneath the southern Lesser  
23  
24  
25  
26 Antilles Arc. *Journal of Petrology* 56(4):815-844  
27

28  
29 Bouilhol P, Schmidt MW, Burg JP (2015) Magma Transfer and Evolution in Channels within  
30 the Arc Crust: the Pyroxenitic Feeder Pipes of Sapat (Kohistan, Pakistan). *Journal of*  
31  
32  
33  
34 *Petrology* 56(7):1309-1342  
35

36  
37 Bouysse P, Westercamp D (1990) Subduction of Atlantic aseismic ridges and Late Cenozoic  
38 evolution of the Lesser Antilles Island-Arc. *Tectonophysics* 175(4):349-380  
39  
40  
41  
42 doi:10.1016/0040-1951(90)90180-g  
43

44  
45 Boynton CH, Westbrook GK, Bott MHP, Long RE (1979) Seismic refraction investigation of  
46 crustal structure beneath the Lesser-Antilles Island Arc. *Geophysical Journal of the Royal*  
47  
48  
49  
50 *Astronomical Society* 58(2):371-393 doi:10.1111/j.1365-246X.1979.tb01031.x  
51

52  
53 Brown G, Holland J, Sigurdsson H, Tomblin J, Arculus R (1977). Geochemistry of the Lesser  
54  
55  
56  
57 Antilles volcanic island arc. *Geochimica Et Cosmochimica Acta* 41(6):785-801  
58  
59  
60  
61  
62  
63  
64  
65

- 1  
2  
3  
4  
5  
6  
7  
8  
9  
10  
11  
12  
13  
14  
15  
16  
17  
18  
19  
20  
21  
22  
23  
24  
25  
26  
27  
28  
29  
30  
31  
32  
33  
34  
35  
36  
37  
38  
39  
40  
41  
42  
43  
44  
45  
46  
47  
48  
49  
50  
51  
52  
53  
54  
55  
56  
57  
58  
59  
60  
61  
62  
63  
64  
65
- Claeson D, Meurer W (2004) Fractional crystallization of hydrous basaltic “arc-type”  
magmas and the formation of amphibole-bearing gabbroic cumulates. *Contributions to  
Mineralogy and Petrology* 147(3):288-304 doi:10.1007/s00410-003-0536-0
- Claiborne LL, Miller CF, Wooden JL (2010) Trace element composition of igneous zircon: a  
thermal and compositional record of the accumulation and evolution of a large silicic  
batholith, Spirit Mountain, Nevada. *Contributions to Mineralogy and Petrology* 160(4):511-  
531 doi:10.1007/s00410-010-0491-5
- Coogan LA, Saunders AD, Kempton PD, Norry MJ (2000) Evidence from oceanic gabbros  
for porous melt migration within a crystal mush beneath the Mid-Atlantic Ridge.  
*Geochemistry, Geophysics, Geosystems* 1:2000GC000072
- Coogan LA, Wilson RN, Gillis KM, MacLeod CJ (2001) Near-solidus evolution of oceanic  
gabbros: Insights from amphibole geochemistry. *Geochimica et Cosmochimica Acta*  
65(23):4339-4357
- Davidson J, Turner S, Handley H, Macpherson C, Dosseto A (2007) Amphibole 'sponge' in  
arc crust? *Geology* 35(9):787-790 doi:10.1130/g23637a.1
- Davidson J, Wilson M (2011) Differentiation and Source Processes at Mt Pelee and the Quill;  
Active Volcanoes in the Lesser Antilles Arc. *Journal of Petrology* 52(7-8):1493-1531  
doi:10.1093/petrology/egq095
- Davidson JP (1983) Lesser Antilles isotopic evidence of the role of subducted sediment in  
island-arc magma genesis. *Nature* 306(5940):253-256 doi:10.1038/306253a0
- Davidson JP (1986) Isotopic and trace-element constraints on the petrogenesis of subduction-  
related lavas from Martinique, Lesser Antilles. *Journal of Geophysical Research-Solid Earth  
and Planets* 91(B6):5943-5962 doi:10.1029/JB091iB06p05943

1 Debari S, Kay SM, Kay RW (1987) Ultramafic xenoliths from Adagdak Volcano, Adak,  
2 Aleutian-Islands, Alaska: Deformed igneous cumulates from the Moho of the island-arc.  
3  
4 Journal of Geology 95(3):329-341  
5

6  
7 Deering CD, Bachmann O (2010) Trace element indicators of crystal accumulation in silicic  
8 igneous rocks. Earth and Planetary Science Letters 297(1–2):324-331  
9

10  
11  
12 Erdmann S, Martel C, Pichavant M, Kushnir A (2014) Amphibole as an archivist of  
13 magmatic crystallization conditions: problems, potential, and implications for inferring  
14 magma storage prior to the paroxysmal 2010 eruption of Mount Merapi, Indonesia.  
15 Contributions to Mineralogy and Petrology 167(6):23 doi:10.1007/s00410-014-1016-4  
16  
17  
18  
19  
20  
21  
22

23 Gaetani GA, Grove TL, Bryan WB (1993) The influence of water on the petrogenesis of  
24 subduction-related igneous rocks. Nature 365(6444):332-334 doi:10.1038/365332a0  
25  
26  
27  
28

29 Germa A, Quidelleur X, Labanieh S, Chauvel C, Lahitte P (2011) The volcanic evolution of  
30 Martinique Island: Insights from K-Ar dating into the Lesser Antilles arc migration since the  
31 Oligocene. Journal of Volcanology and Geothermal Research 208(3-4):122-135  
32  
33  
34  
35  
36  
37  
38  
39  
40  
41  
42  
43  
44  
45  
46  
47  
48  
49  
50  
51  
52  
53  
54  
55  
56  
57  
58  
59  
60  
61  
62  
63  
64  
65

66  
67  
68  
69  
70  
71  
72  
73  
74  
75  
76  
77  
78  
79  
80  
81  
82  
83  
84  
85  
86  
87  
88  
89  
90  
91  
92  
93  
94  
95  
96  
97  
98  
99  
100  
101  
102  
103  
104  
105  
106  
107  
108  
109  
110  
111  
112  
113  
114  
115  
116  
117  
118  
119  
120  
121  
122  
123  
124  
125  
126  
127  
128  
129  
130  
131  
132  
133  
134  
135  
136  
137  
138  
139  
140  
141  
142  
143  
144  
145  
146  
147  
148  
149  
150  
151  
152  
153  
154  
155  
156  
157  
158  
159  
160  
161  
162  
163  
164  
165  
166  
167  
168  
169  
170  
171  
172  
173  
174  
175  
176  
177  
178  
179  
180  
181  
182  
183  
184  
185  
186  
187  
188  
189  
190  
191  
192  
193  
194  
195  
196  
197  
198  
199  
200  
201  
202  
203  
204  
205  
206  
207  
208  
209  
210  
211  
212  
213  
214  
215  
216  
217  
218  
219  
220  
221  
222  
223  
224  
225  
226  
227  
228  
229  
230  
231  
232  
233  
234  
235  
236  
237  
238  
239  
240  
241  
242  
243  
244  
245  
246  
247  
248  
249  
250  
251  
252  
253  
254  
255  
256  
257  
258  
259  
260  
261  
262  
263  
264  
265  
266  
267  
268  
269  
270  
271  
272  
273  
274  
275  
276  
277  
278  
279  
280  
281  
282  
283  
284  
285  
286  
287  
288  
289  
290  
291  
292  
293  
294  
295  
296  
297  
298  
299  
300  
301  
302  
303  
304  
305  
306  
307  
308  
309  
310  
311  
312  
313  
314  
315  
316  
317  
318  
319  
320  
321  
322  
323  
324  
325  
326  
327  
328  
329  
330  
331  
332  
333  
334  
335  
336  
337  
338  
339  
340  
341  
342  
343  
344  
345  
346  
347  
348  
349  
350  
351  
352  
353  
354  
355  
356  
357  
358  
359  
360  
361  
362  
363  
364  
365  
366  
367  
368  
369  
370  
371  
372  
373  
374  
375  
376  
377  
378  
379  
380  
381  
382  
383  
384  
385  
386  
387  
388  
389  
390  
391  
392  
393  
394  
395  
396  
397  
398  
399  
400  
401  
402  
403  
404  
405  
406  
407  
408  
409  
410  
411  
412  
413  
414  
415  
416  
417  
418  
419  
420  
421  
422  
423  
424  
425  
426  
427  
428  
429  
430  
431  
432  
433  
434  
435  
436  
437  
438  
439  
440  
441  
442  
443  
444  
445  
446  
447  
448  
449  
450  
451  
452  
453  
454  
455  
456  
457  
458  
459  
460  
461  
462  
463  
464  
465  
466  
467  
468  
469  
470  
471  
472  
473  
474  
475  
476  
477  
478  
479  
480  
481  
482  
483  
484  
485  
486  
487  
488  
489  
490  
491  
492  
493  
494  
495  
496  
497  
498  
499  
500  
501  
502  
503  
504  
505  
506  
507  
508  
509  
510  
511  
512  
513  
514  
515  
516  
517  
518  
519  
520  
521  
522  
523  
524  
525  
526  
527  
528  
529  
530  
531  
532  
533  
534  
535  
536  
537  
538  
539  
540  
541  
542  
543  
544  
545  
546  
547  
548  
549  
550  
551  
552  
553  
554  
555  
556  
557  
558  
559  
560  
561  
562  
563  
564  
565  
566  
567  
568  
569  
570  
571  
572  
573  
574  
575  
576  
577  
578  
579  
580  
581  
582  
583  
584  
585  
586  
587  
588  
589  
590  
591  
592  
593  
594  
595  
596  
597  
598  
599  
600  
601  
602  
603  
604  
605  
606  
607  
608  
609  
610  
611  
612  
613  
614  
615  
616  
617  
618  
619  
620  
621  
622  
623  
624  
625  
626  
627  
628  
629  
630  
631  
632  
633  
634  
635  
636  
637  
638  
639  
640  
641  
642  
643  
644  
645  
646  
647  
648  
649  
650  
651  
652  
653  
654  
655  
656  
657  
658  
659  
660  
661  
662  
663  
664  
665  
666  
667  
668  
669  
670  
671  
672  
673  
674  
675  
676  
677  
678  
679  
680  
681  
682  
683  
684  
685  
686  
687  
688  
689  
690  
691  
692  
693  
694  
695  
696  
697  
698  
699  
700  
701  
702  
703  
704  
705  
706  
707  
708  
709  
710  
711  
712  
713  
714  
715  
716  
717  
718  
719  
720  
721  
722  
723  
724  
725  
726  
727  
728  
729  
730  
731  
732  
733  
734  
735  
736  
737  
738  
739  
740  
741  
742  
743  
744  
745  
746  
747  
748  
749  
750  
751  
752  
753  
754  
755  
756  
757  
758  
759  
760  
761  
762  
763  
764  
765  
766  
767  
768  
769  
770  
771  
772  
773  
774  
775  
776  
777  
778  
779  
780  
781  
782  
783  
784  
785  
786  
787  
788  
789  
790  
791  
792  
793  
794  
795  
796  
797  
798  
799  
800  
801  
802  
803  
804  
805  
806  
807  
808  
809  
810  
811  
812  
813  
814  
815  
816  
817  
818  
819  
820  
821  
822  
823  
824  
825  
826  
827  
828  
829  
830  
831  
832  
833  
834  
835  
836  
837  
838  
839  
840  
841  
842  
843  
844  
845  
846  
847  
848  
849  
850  
851  
852  
853  
854  
855  
856  
857  
858  
859  
860  
861  
862  
863  
864  
865  
866  
867  
868  
869  
870  
871  
872  
873  
874  
875  
876  
877  
878  
879  
880  
881  
882  
883  
884  
885  
886  
887  
888  
889  
890  
891  
892  
893  
894  
895  
896  
897  
898  
899  
900  
901  
902  
903  
904  
905  
906  
907  
908  
909  
910  
911  
912  
913  
914  
915  
916  
917  
918  
919  
920  
921  
922  
923  
924  
925  
926  
927  
928  
929  
930  
931  
932  
933  
934  
935  
936  
937  
938  
939  
940  
941  
942  
943  
944  
945  
946  
947  
948  
949  
950  
951  
952  
953  
954  
955  
956  
957  
958  
959  
960  
961  
962  
963  
964  
965  
966  
967  
968  
969  
970  
971  
972  
973  
974  
975  
976  
977  
978  
979  
980  
981  
982  
983  
984  
985  
986  
987  
988  
989  
990  
991  
992  
993  
994  
995  
996  
997  
998  
999  
1000

Heath E, Macdonald R, Belkin H, Hawkesworth C, Sigurdsson H (1998) Magmagenesis at  
Soufriere Volcano, St Vincent, Lesser Antilles Arc. Journal of Petrology 39(10):1721-1764

1 Holland T, Blundy J (1994) Non-ideal interactions in calcic amphiboles and their bearing on  
2 amphibole-plagioclase thermometry. *Contributions to Mineralogy and Petrology* 116(4):433-  
3  
4 447 doi:10.1007/bf00310910  
5  
6

7 Holness MB (2005) Spatial constraints on magma chamber replenishment events from  
8  
9 textural observations of cumulates: The Rum layered intrusion, Scotland. *Journal of Petrology*  
10  
11 46(8):1585-1601 doi:10.1093/petrology/egi027  
12  
13

14 Holness MB, Hallworth MA, Woods A, Sides RE (2007) Infiltration metasomatism of  
15  
16 cumulates by intrusive magma replenishment: The Wavy Horizon, Isle of Rum, Scotland.  
17  
18 *Journal of Petrology* 48(3):563-587 doi:10.1093/petrology/egl072  
19  
20  
21

22 Irvine TN (1974) Petrology of the Duke Island ultramafic complex southeastern Alaska.  
23  
24 *Geological Society of America Memoirs* 138:1-244  
25  
26

27 Kiddle EJ, Edwards BR, Loughlin SC, Petterson M, Sparks RSJ (2010) Crustal structure  
28  
29 beneath Montserrat, Lesser Antilles, constrained by xenoliths, seismic velocity structure and  
30  
31 petrology. *Geophysical Research Letters* 31, L00E11  
32  
33  
34

35 Kodaira S, Sato T, Takahashi N, Miura S, Tamura Y, Tatsumi Y, Kaneda Y (2007) New  
36  
37 seismological constraints on growth of continental crust in the Izu-Bonin intra-oceanic arc.  
38  
39  
40 *Geology* 35(11):1031-1034 doi:10.1130/g23901a.1  
41  
42  
43

44 Labanieh S, Chauvel C, Germa A, Quidelleur X (2012) Martinique: a Clear Case for  
45  
46 Sediment Melting and Slab Dehydration as a Function of Distance to the Trench. *Journal of*  
47  
48 *Petrology* 53(12):2441-2464 doi:10.1093/petrology/egs055  
49  
50  
51

52 Leake BE, Woolley AR, Birch WD, Burke EAJ, Ferraris G, Grice JD, Hawthorne FC, Kisch  
53  
54 HJ, Krivovichev VG, Schumacher JC, Stephenson NCN, Whittaker EJW (2003)  
55  
56  
57 *Nomenclature of amphiboles: Additions and revisions to the International Mineralogical*  
58  
59  
60  
61  
62  
63  
64  
65

1 Association's 1997 recommendations. *Canadian Mineralogist* 41:1355-1362

2 doi:10.2113/gscanmin.41.6.1355

3  
4  
5 Leuthold J, Blundy JD, Holness MB, Sides R (2014) Successive episodes of reactive liquid  
6 flow through a layered intrusion (Unit 9, Rum Eastern Layered Intrusion, Scotland).

7  
8  
9 Contributions to Mineralogy and Petrology 168:1021

10  
11  
12  
13 Lewis JF (1973) Mineralogy of the ejected plutonic blocks of the Soufriere Volcano St.

14  
15 Vincent: olivine, pyroxene, amphibole and magnetite paragenesis. Contributions to  
16 Mineralogy and Petrology 38:197–220

17  
18  
19  
20  
21 Macdonald R, Hawkesworth CJ, Heath E (2000) The Lesser Antilles volcanic chain: a study  
22 in arc magmatism. *Earth-Science Reviews* 49(1-4):1-76 doi:10.1016/s0012-8252(99)00069-0

23  
24  
25  
26  
27 Mandler BE, Grove TL (2016) Controls on the stability and composition of amphibole in the  
28 Earth's mantle. *Contributions to Mineralogy and Petrology* 171(8-9):68

29  
30  
31  
32  
33 Martel C, Pichavant M, Holtz F, Scaillet B, Bourdier JL, Traineau H (1999) Effects of f(O<sub>2</sub>)  
34 and H<sub>2</sub>O on andesite phase relations between 2 and 4 kbar. *Journal of Geophysical Research-*  
35  
36  
37  
38  
39  
40  
41  
42  
43  
44  
45  
46  
47  
48  
49  
50  
51  
52  
53  
54  
55  
56  
57  
58  
59  
60  
61  
62  
63  
64  
65  
66  
67  
68  
69  
70  
71  
72  
73  
74  
75  
76  
77  
78  
79  
80  
81  
82  
83  
84  
85  
86  
87  
88  
89  
90  
91  
92  
93  
94  
95  
96  
97  
98  
99  
100  
101  
102  
103  
104  
105  
106  
107  
108  
109  
110  
111  
112  
113  
114  
115  
116  
117  
118  
119  
120  
121  
122  
123  
124  
125  
126  
127  
128  
129  
130  
131  
132  
133  
134  
135  
136  
137  
138  
139  
140  
141  
142  
143  
144  
145  
146  
147  
148  
149  
150  
151  
152  
153  
154  
155  
156  
157  
158  
159  
160  
161  
162  
163  
164  
165  
166  
167  
168  
169  
170  
171  
172  
173  
174  
175  
176  
177  
178  
179  
180  
181  
182  
183  
184  
185  
186  
187  
188  
189  
190  
191  
192  
193  
194  
195  
196  
197  
198  
199  
200  
201  
202  
203  
204  
205  
206  
207  
208  
209  
210  
211  
212  
213  
214  
215  
216  
217  
218  
219  
220  
221  
222  
223  
224  
225  
226  
227  
228  
229  
230  
231  
232  
233  
234  
235  
236  
237  
238  
239  
240  
241  
242  
243  
244  
245  
246  
247  
248  
249  
250  
251  
252  
253  
254  
255  
256  
257  
258  
259  
260  
261  
262  
263  
264  
265  
266  
267  
268  
269  
270  
271  
272  
273  
274  
275  
276  
277  
278  
279  
280  
281  
282  
283  
284  
285  
286  
287  
288  
289  
290  
291  
292  
293  
294  
295  
296  
297  
298  
299  
300  
301  
302  
303  
304  
305  
306  
307  
308  
309  
310  
311  
312  
313  
314  
315  
316  
317  
318  
319  
320  
321  
322  
323  
324  
325  
326  
327  
328  
329  
330  
331  
332  
333  
334  
335  
336  
337  
338  
339  
340  
341  
342  
343  
344  
345  
346  
347  
348  
349  
350  
351  
352  
353  
354  
355  
356  
357  
358  
359  
360  
361  
362  
363  
364  
365  
366  
367  
368  
369  
370  
371  
372  
373  
374  
375  
376  
377  
378  
379  
380  
381  
382  
383  
384  
385  
386  
387  
388  
389  
390  
391  
392  
393  
394  
395  
396  
397  
398  
399  
400  
401  
402  
403  
404  
405  
406  
407  
408  
409  
410  
411  
412  
413  
414  
415  
416  
417  
418  
419  
420  
421  
422  
423  
424  
425  
426  
427  
428  
429  
430  
431  
432  
433  
434  
435  
436  
437  
438  
439  
440  
441  
442  
443  
444  
445  
446  
447  
448  
449  
450  
451  
452  
453  
454  
455  
456  
457  
458  
459  
460  
461  
462  
463  
464  
465  
466  
467  
468  
469  
470  
471  
472  
473  
474  
475  
476  
477  
478  
479  
480  
481  
482  
483  
484  
485  
486  
487  
488  
489  
490  
491  
492  
493  
494  
495  
496  
497  
498  
499  
500  
501  
502  
503  
504  
505  
506  
507  
508  
509  
510  
511  
512  
513  
514  
515  
516  
517  
518  
519  
520  
521  
522  
523  
524  
525  
526  
527  
528  
529  
530  
531  
532  
533  
534  
535  
536  
537  
538  
539  
540  
541  
542  
543  
544  
545  
546  
547  
548  
549  
550  
551  
552  
553  
554  
555  
556  
557  
558  
559  
560  
561  
562  
563  
564  
565  
566  
567  
568  
569  
570  
571  
572  
573  
574  
575  
576  
577  
578  
579  
580  
581  
582  
583  
584  
585  
586  
587  
588  
589  
590  
591  
592  
593  
594  
595  
596  
597  
598  
599  
600  
601  
602  
603  
604  
605  
606  
607  
608  
609  
610  
611  
612  
613  
614  
615  
616  
617  
618  
619  
620  
621  
622  
623  
624  
625  
626  
627  
628  
629  
630  
631  
632  
633  
634  
635  
636  
637  
638  
639  
640  
641  
642  
643  
644  
645  
646  
647  
648  
649  
650  
651  
652  
653  
654  
655  
656  
657  
658  
659  
660  
661  
662  
663  
664  
665  
666  
667  
668  
669  
670  
671  
672  
673  
674  
675  
676  
677  
678  
679  
680  
681  
682  
683  
684  
685  
686  
687  
688  
689  
690  
691  
692  
693  
694  
695  
696  
697  
698  
699  
700  
701  
702  
703  
704  
705  
706  
707  
708  
709  
710  
711  
712  
713  
714  
715  
716  
717  
718  
719  
720  
721  
722  
723  
724  
725  
726  
727  
728  
729  
730  
731  
732  
733  
734  
735  
736  
737  
738  
739  
740  
741  
742  
743  
744  
745  
746  
747  
748  
749  
750  
751  
752  
753  
754  
755  
756  
757  
758  
759  
760  
761  
762  
763  
764  
765  
766  
767  
768  
769  
770  
771  
772  
773  
774  
775  
776  
777  
778  
779  
780  
781  
782  
783  
784  
785  
786  
787  
788  
789  
790  
791  
792  
793  
794  
795  
796  
797  
798  
799  
800  
801  
802  
803  
804  
805  
806  
807  
808  
809  
810  
811  
812  
813  
814  
815  
816  
817  
818  
819  
820  
821  
822  
823  
824  
825  
826  
827  
828  
829  
830  
831  
832  
833  
834  
835  
836  
837  
838  
839  
840  
841  
842  
843  
844  
845  
846  
847  
848  
849  
850  
851  
852  
853  
854  
855  
856  
857  
858  
859  
860  
861  
862  
863  
864  
865  
866  
867  
868  
869  
870  
871  
872  
873  
874  
875  
876  
877  
878  
879  
880  
881  
882  
883  
884  
885  
886  
887  
888  
889  
890  
891  
892  
893  
894  
895  
896  
897  
898  
899  
900  
901  
902  
903  
904  
905  
906  
907  
908  
909  
910  
911  
912  
913  
914  
915  
916  
917  
918  
919  
920  
921  
922  
923  
924  
925  
926  
927  
928  
929  
930  
931  
932  
933  
934  
935  
936  
937  
938  
939  
940  
941  
942  
943  
944  
945  
946  
947  
948  
949  
950  
951  
952  
953  
954  
955  
956  
957  
958  
959  
960  
961  
962  
963  
964  
965  
966  
967  
968  
969  
970  
971  
972  
973  
974  
975  
976  
977  
978  
979  
980  
981  
982  
983  
984  
985  
986  
987  
988  
989  
990  
991  
992  
993  
994  
995  
996  
997  
998  
999  
1000

40  
41  
42  
43  
44  
45  
46  
47  
48  
49  
50  
51  
52  
53  
54  
55  
56  
57  
58  
59  
60  
61  
62  
63  
64  
65  
66  
67  
68  
69  
70  
71  
72  
73  
74  
75  
76  
77  
78  
79  
80  
81  
82  
83  
84  
85  
86  
87  
88  
89  
90  
91  
92  
93  
94  
95  
96  
97  
98  
99  
100  
101  
102  
103  
104  
105  
106  
107  
108  
109  
110  
111  
112  
113  
114  
115  
116  
117  
118  
119  
120  
121  
122  
123  
124  
125  
126  
127  
128  
129  
130  
131  
132  
133  
134  
135  
136  
137  
138  
139  
140  
141  
142  
143  
144  
145  
146  
147  
148  
149  
150  
151  
152  
153  
154  
155  
156  
157  
158  
159  
160  
161  
162  
163  
164  
165  
166  
167  
168  
169  
170  
171  
172  
173  
174  
175  
176  
177  
178  
179  
180  
181  
182  
183  
184  
185  
186  
187  
188  
189  
190  
191  
192  
193  
194  
195  
196  
197  
198  
199  
200  
201  
202  
203  
204  
205  
206  
207  
208  
209  
210  
211  
212  
213  
214  
215  
216  
217  
218  
219  
220  
221  
222  
223  
224  
225  
226  
227  
228  
229  
230  
231  
232  
233  
234  
235  
236  
237  
238  
239  
240  
241  
242  
243  
244  
245  
246  
247  
248  
249  
250  
251  
252  
253  
254  
255  
256  
257  
258  
259  
260  
261  
262  
263  
264  
265  
266  
267  
268  
269  
270  
271  
272  
273  
274  
275  
276  
277  
278  
279  
280  
281  
282  
283  
284  
285  
286  
287  
288  
289  
290  
291  
292  
293  
294  
295  
296  
297  
298  
299  
300  
301  
302  
303  
304  
305  
306  
307  
308  
309  
310  
311  
312  
313  
314  
315  
316  
317  
318  
319  
320  
321  
322  
323  
324  
325  
326  
327  
328  
329  
330  
331  
332  
333  
334  
335  
336  
337  
338  
339  
340  
341  
342  
343  
344  
345  
346  
347  
348  
349  
350  
351  
352  
353  
354  
355  
356  
357  
358  
359  
360  
361  
362  
363  
364  
365  
366  
367  
368  
369  
370  
371  
372  
373  
374  
375  
376  
377  
378  
379  
380  
381  
382  
383  
384  
385  
386  
387  
388  
389  
390  
391  
392  
393  
394  
395  
396  
397  
398  
399  
400  
401  
402  
403  
404  
405  
406  
407  
408  
409  
410  
411  
412  
413  
414  
415  
416  
417  
418  
419  
420  
421  
422  
423  
424  
425  
426  
427  
428  
429  
430  
431  
432  
433  
434  
435  
436  
437  
438  
439  
440  
441  
442  
443  
444  
445  
446  
447  
448  
449  
450  
451  
452  
453  
454  
455  
456  
457  
458  
459  
460  
461  
462  
463  
464  
465  
466  
467  
468  
469  
470  
471  
472  
473  
474  
475  
476  
477  
478  
479  
480  
481  
482  
483  
484  
485  
486  
487  
488  
489  
490  
491  
492  
493  
494  
495  
496  
497  
498  
499  
500  
501  
502  
503  
504  
505  
506  
507  
508  
509  
510  
511  
512  
513  
514  
515  
516  
517  
518  
519  
520  
521  
522  
523  
524  
525  
526  
527  
528  
529  
530  
531  
532  
533  
534  
535  
536  
537  
538  
539  
540  
541  
542  
543  
544  
545  
546  
547  
548  
549  
550  
551  
552  
553  
554  
555  
556  
557  
558  
559  
560  
561  
562  
563  
564  
565  
566  
567  
568  
569  
570  
571  
572  
573  
574  
575  
576  
577  
578  
579  
580  
581  
582  
583  
584  
585  
586  
587  
588  
589  
590  
591  
592  
593  
594  
595  
596  
597  
598  
599  
600  
601  
602  
603  
604  
605  
606  
607  
608  
609  
610  
611  
612  
613  
614  
615  
616  
617  
618  
619  
620  
621  
622  
623  
624  
625  
626  
627  
628  
629  
630  
631  
632  
633  
634  
635  
636  
637  
638  
639  
640  
641  
642  
643  
644  
645  
646  
647  
648  
649  
650  
651  
652  
653  
654  
655  
656  
657  
658  
659  
660  
661  
662  
663  
664  
665  
666  
667  
668  
669  
670  
671  
672  
673  
674  
675  
676  
677  
678  
679  
680  
681  
682  
683  
684  
685  
686  
687  
688  
689  
690  
691  
692  
693  
694  
695  
696  
697  
698  
699  
700  
701  
702  
703  
704  
705  
706  
707  
708  
709  
710  
711  
712  
713  
714  
715  
716  
717  
718  
719  
720  
721  
722  
723  
724  
725  
726  
727  
728  
729  
730  
731  
732  
733  
734  
735  
736  
737  
738  
739  
740  
741  
742  
743  
744  
745  
746  
747  
748  
749  
750  
751  
752  
753  
754  
755  
756  
757  
758  
759  
760  
761  
762  
763  
764  
765  
766  
767  
768  
769  
770  
771  
772  
773  
774  
775  
776  
777  
778  
779  
780  
781  
782  
783  
784  
785  
786  
787  
788  
789  
790  
791  
792  
793  
794  
795  
796  
797  
798  
799  
800  
801  
802  
803  
804  
805  
806  
807  
808  
809  
810  
811  
812  
813  
814  
815  
816  
817  
818  
819  
820  
821  
822  
823  
824  
825  
826  
827  
828  
829  
830  
831  
832  
833  
834  
835  
836  
837  
838  
839  
840  
841  
842  
843  
844  
845  
846  
847  
848  
849  
850  
851  
852  
853  
854  
855  
856  
857  
858  
859  
860  
861  
862  
863  
864  
865  
866  
867  
868  
869  
870  
871  
872  
873  
874  
875  
876  
877  
878  
879  
880  
881  
882  
883  
884  
885  
886  
887  
888  
889  
890  
891  
892  
893  
894  
895  
896  
897  
898  
899  
900  
901  
902  
903  
904  
905  
906  
907  
908  
909  
910  
911  
912  
913  
914  
915  
916  
917  
918  
919  
920  
921  
922  
923  
924  
925  
926  
927  
928  
929  
930  
931  
932  
933  
934  
935  
936  
937  
938  
939  
940  
941  
942  
943  
944  
945  
946  
947  
948  
949  
950  
951  
952  
953  
954  
955  
956  
957  
958  
959  
960  
961  
962  
963  
964  
965  
966  
967  
968  
969  
970  
971  
972  
973  
974  
975  
976  
977  
978  
979  
980  
981  
982  
983  
984  
985  
986  
987  
988  
989  
990  
991  
992  
993  
994  
995  
996  
997  
998  
999  
1000

10  
11  
12  
13  
14  
15  
16  
17  
18  
19  
20  
21  
22  
23  
24  
25  
26  
27  
28  
29  
30  
31  
32  
33  
34  
35  
36  
37  
38  
39  
40  
41  
42  
43  
44  
45  
46  
47  
48  
49  
50  
51  
52  
53  
54  
55  
56  
57  
58  
59  
60  
61  
62  
63  
64  
65  
66  
67  
68  
69  
70  
71  
72  
73  
74  
75  
76  
77  
78  
79  
80  
81  
82  
83  
84  
85  
86  
87  
88  
89  
90  
91  
92  
93  
94  
95  
96  
97  
98  
99  
100  
101  
102  
103  
104  
105  
106  
107  
108  
109  
110  
111  
112  
113  
114  
115  
116  
117  
118  
119  
120  
121  
122  
123  
124  
125  
126  
127  
128  
129  
130  
131  
132  
133  
134  
135  
136  
137  
138  
139  
140  
141  
142  
143  
144  
145  
146  
147  
148  
149  
150  
151  
152  
153  
154  
155  
156  
157  
158  
159  
160  
161  
162  
163  
164  
165  
166  
167  
168  
169  
170  
171  
172  
173  
174  
175  
176  
177  
178  
179  
180  
181  
182  
183  
184  
185  
186  
187  
188  
189  
190  
191  
192  
193  
194  
195  
196  
197  
198  
199  
200  
201  
202  
203  
204  
205  
206  
207  
208  
209  
210  
211  
212  
213  
214  
215  
216  
217  
218  
219  
220  
221  
222  
223  
224  
225  
226  
227  
228  
229  
230  
231  
232  
233  
234  
235  
236  
237  
238  
239  
240  
241  
242  
243  
244  
245  
246  
247  
248  
249  
250  
251  
252  
253  
254  
255  
256  
257  
258  
259  
260  
261  
262  
263  
264  
265  
266  
267  
268  
269  
270  
271  
272  
273  
274  
275  
276  
277  
278  
279  
280  
281  
282  
283  
284  
285  
286  
287  
288  
289  
290  
291  
292  
293  
294  
295  
296  
297  
298  
299  
300  
301  
302  
303  
304  
305  
306  
307  
308  
309  
310  
311  
312  
313  
314  
315  
316  
317  
318  
319  
320  
321  
322  
323  
324  
325  
326  
327  
328  
329  
330  
331  
332  
333  
334  
335  
336  
337  
338  
339  
340  
341  
342  
343  
344  
345  
346  
347  
348  
349  
350  
351  
352  
353  
354  
355  
356  
357  
358  
359  
360  
361  
362  
363  
364  
365  
366  
367  
368  
369  
370  
371  
372  
373  
374  
375  
376  
377  
378  
379  
380  
381  
382  
383  
384  
385  
386  
387  
388  
389  
390  
391  
392  
393  
394  
395  
396  
397  
398  
399  
400  
401  
402  
403  
404  
405  
406  
407  
408  
409  
410  
411  
412  
413  
414  
415  
416  
417  
418  
419  
420  
421  
422  
423  
424  
425  
426  
427  
428  
429

1 Melekhova E, Blundy J, Robertson R, Humphreys MCS (2015) Experimental Evidence for  
2 Polybaric Differentiation of Primitive Arc Basalt beneath St. Vincent, Lesser Antilles. Journal  
3 of Petrology 56(1):161-192 doi:10.1093/petrology/egu074  
4  
5

6  
7 Meurer WP, Claeson DT (2002) Evolution of Crystallizing Interstitial Liquid in an Arc-  
8 Related Cumulate Determined by LA ICP-MS Mapping of a Large Amphibole Oikocryst.  
9 Journal of Petrology 43(4):607-629  
10  
11

12 Morse SA (1996) Kiglapait mineralogy III: olivine compositions and Rayleigh fractionation  
13 models. Journal of Petrology 37(5):1037–1061  
14  
15

16 Murray CG (1972) Zoned Ultramafic Complexes of the Alaskan Type: Feeder Pipes of  
17 Andesitic Volcanoes. GSA Memoirs 132:313-336  
18  
19

20  
21 Nandedkar RH, Hürlimann N, Ulmer P, Müntener O (2016) Amphibole–melt trace element  
22 partitioning of fractionating calc-alkaline magmas in the lower crust: an experimental study.  
23 Contributions to Mineralogy and Petrology 171: 71  
24  
25

26  
27 Niida K, Green DH (1999) Stability and chemical composition of pargasitic amphibole in  
28 MORB pyroxene under upper mantle conditions. Contributions to Mineralogy and Petrology  
29 135(1):18-40  
30  
31

32  
33  
34  
35  
36  
37  
38  
39  
40  
41  
42  
43  
44  
45  
46  
47  
48  
49  
50  
51  
52  
53  
54  
55  
56  
57  
58  
59  
60  
61  
62  
63  
64  
65

Palme H, O'Neill HSC (2003) Cosmochemical estimates of mantle composition. Treatise on  
geochemistry 2:1-38

Passmore E, Maclennan J, Fitton G, Thordarson T (2012) Mush Disaggregation in Basaltic  
Magma Chambers: Evidence from the AD 1783 Laki Eruption. Journal of Petrology  
53(12):2593-2623

Philpotts JA (1970) Redox estimation from a calculation of  $\text{Eu}^{2+}$  and  $\text{Eu}^{3+}$  concentrations in  
natural phases. Earth and Planetary Science Letters 9(3):257-268

1 Pichavant M, Macdonald R (2007) Crystallization of primitive basaltic magmas at crustal  
2 pressures and genesis of the calc-alkaline igneous suite: experimental evidence from St  
3 Vincent, Lesser Antilles arc. *Contributions to Mineralogy and Petrology* 154(5):535-558  
4  
5 doi:10.1007/s00410-007-0208-6  
6  
7

8  
9  
10 Pichavant M, Mysen BO, Macdonald R (2002) Source and H<sub>2</sub>O content of high-MgO  
11 magmas in island arc settings: An experimental study of a primitive calc-alkaline basalt from  
12 St. Vincent, Lesser Antilles arc. *Geochimica Et Cosmochimica Acta* 66(12):2193-2209  
13  
14 doi:10.1016/s0016-7037(01)00891-2  
15  
16  
17

18  
19  
20 Putirka K (2016) Amphibole thermometers and barometers for igneous systems and some  
21 implications for eruption mechanisms of felsic magmas at arc volcanoes. *American*  
22  
23 *Mineralogist* 101:841-858  
24  
25

26  
27  
28 Reiners PW (1998) Reactive melt transport in the mantle and geochemical signatures of  
29 mantle-derived magmas. *Journal of Petrology* 39(5):1039-1061  
30  
31 doi:10.1093/petrology/39.5.1039  
32  
33  
34

35  
36 Ridolfi F, Renzulli A (2012) Calcic amphiboles in calc-alkaline and alkaline magmas:  
37 thermobarometric and chemometric empirical equations valid up to 1,130A degrees C and 2.2  
38 GPa. *Contributions to Mineralogy and Petrology* 163(5):877-895 doi:10.1007/s00410-011-  
39  
40 0704-6  
41  
42  
43

44  
45  
46 Ridolfi F, Renzulli A, Puerini M (2010) Stability and chemical equilibrium of amphibole in  
47 calc-alkaline magmas: an overview, new thermobarometric formulations and application to  
48 subduction-related volcanoes. *Contributions to Mineralogy and Petrology* 160(1):45-66  
49  
50  
51 doi:10.1007/s00410-009-0465-7  
52  
53  
54

55  
56 Sawyer EW (1994) Melt segregation in the continental crust. *Geology* 22(11):1019-1022  
57  
58  
59  
60  
61  
62  
63  
64  
65

1 Schiano P, Eiler JM, Hutcheon ID, Stolper EM (2000) Primitive CaO-rich, silica-  
2 undersaturated melts in island arcs: Evidence for the involvement of clinopyroxene-rich  
3 lithologies in the petrogenesis of arc magmas. *Geochemistry, Geophysics, Geosystems* 1(5)  
4  
5  
6  
7  
8 Schlaphorst D, Kendall JM, Blundy JD, Melekhova E, Baptie B, Latchman JL, Bouin MP,  
9  
10 Tait S (2014) Observations and modeling of the crustal structure and Moho strength variation  
11 along the Lesser Antilles Arc. American Geophysical Union, Fall Meeting 2014, abstract  
12  
13 2014AGUFM.T53E..07S  
14  
15  
16  
17  
18 Sisson TW (1994) Hornblende-melt trace-element partitioning measured by Ion Microprobe.  
19  
20 *Chemical Geology* 117(1-4):331-344 doi:10.1016/0009-2541(94)90135-x  
21  
22  
23  
24 Sisson TW, Grove TL (1993a) Experimental investigations of the role of H<sub>2</sub>O in calc-alkaline  
25 differentiation and subduction zone magmatism. *Contributions to Mineralogy and Petrology*  
26 113(2):143-166 doi:10.1007/bf00283225  
27  
28  
29  
30  
31 Sisson TW, Grove TL (1993b) Temperatures and H<sub>2</sub>O contents of low-MgO high-alumina  
32 basalts. *Contributions to Mineralogy and Petrology* 113(2):167-184 doi:10.1007/bf00283226  
33  
34  
35  
36  
37 Smith AL, Roobol MJ, Gunn BM (1980) The Lesser Antilles-A discussion of the Island arc  
38 magmatism. *Bulletin Volcanologique* 43(2):287-302  
39  
40  
41  
42  
43 Smith DJ (2014) Clinopyroxene precursors to amphibole sponges in arc crust. *Nature*  
44  
45 *Communications* 5:6 doi:10.1038/ncomms5329  
46  
47  
48  
49 Solano JMS, Jackson MD, Sparks RSJ, Blundy J (2014) Evolution of major and trace element  
50 composition during melt migration through crystalline mush: Implications for chemical  
51 differentiation in the crust. *American Journal of Science* 314(5):895-939  
52  
53  
54  
55  
56 doi:10.2475/05.2014.01  
57  
58  
59  
60  
61  
62  
63  
64  
65

1 Solano JMS, Jackson MD, Sparks RSJ, Blundy JD, Annen C (2012) Melt Segregation in  
2 Deep Crustal Hot Zones: a Mechanism for Chemical Differentiation, Crustal Assimilation and  
3 the Formation of Evolved Magmas. *Journal of Petrology* 53(10):1999-2026  
4

5 doi:10.1093/petrology/egs041  
6

7  
8  
9  
10 Stamper CC, Blundy JD, Arculus RJ, Melekhova E (2014) Petrology of Plutonic Xenoliths  
11 and Volcanic Rocks from Grenada, Lesser Antilles. *Journal of Petrology* 55(7):1353-1387  
12

13 doi:10.1093/petrology/egu027  
14

15  
16  
17 Stuart CA, Piazzolo S, Daczko NR (2016) Mass transfer in the lower crust: Evidence for  
18 incipient melt assisted flow along grain boundaries in the deep arc granulites of Fiordland,  
19 New Zealand. *Geochemistry, Geophysics, Geosystems*. Accepted Author Manuscript.  
20

21 doi:10.1002/2015GC006236  
22

23  
24  
25 Streckeisen A (1976) To each plutonic rock its proper name. *Earth-Science Reviews* 12(1):1-  
26 33 doi:10.1016/0012-8252(76)90052-0  
27

28  
29  
30 Tamura Y, Gill JB, Tollstrup D, Kawabata H, Shukuno H, Chang Q, Miyazaki T, Takahashi  
31 T, Hirahara Y, Kodaira S, Ishizuka O, Suzuki T, Kido Y, Fiske RS, Tatsumi Y (2009) Silicic  
32 Magmas in the Izu–Bonin Oceanic Arc and Implications for Crustal Evolution. *Journal of*  
33  
34  
35  
36  
37  
38  
39  
40  
41  
42  
43  
44  
45  
46  
47  
48  
49  
50  
51  
52  
53  
54  
55  
56  
57  
58  
59  
60  
61  
62  
63  
64  
65

66  
67  
68  
69  
70  
71  
72  
73  
74  
75  
76  
77  
78  
79  
80  
81  
82  
83  
84  
85  
86  
87  
88  
89  
90  
91  
92  
93  
94  
95  
96  
97  
98  
99  
100  
101  
102  
103  
104  
105  
106  
107  
108  
109  
110  
111  
112  
113  
114  
115  
116  
117  
118  
119  
120  
121  
122  
123  
124  
125  
126  
127  
128  
129  
130  
131  
132  
133  
134  
135  
136  
137  
138  
139  
140  
141  
142  
143  
144  
145  
146  
147  
148  
149  
150  
151  
152  
153  
154  
155  
156  
157  
158  
159  
160  
161  
162  
163  
164  
165  
166  
167  
168  
169  
170  
171  
172  
173  
174  
175  
176  
177  
178  
179  
180  
181  
182  
183  
184  
185  
186  
187  
188  
189  
190  
191  
192  
193  
194  
195  
196  
197  
198  
199  
200  
201  
202  
203  
204  
205  
206  
207  
208  
209  
210  
211  
212  
213  
214  
215  
216  
217  
218  
219  
220  
221  
222  
223  
224  
225  
226  
227  
228  
229  
230  
231  
232  
233  
234  
235  
236  
237  
238  
239  
240  
241  
242  
243  
244  
245  
246  
247  
248  
249  
250  
251  
252  
253  
254  
255  
256  
257  
258  
259  
260  
261  
262  
263  
264  
265  
266  
267  
268  
269  
270  
271  
272  
273  
274  
275  
276  
277  
278  
279  
280  
281  
282  
283  
284  
285  
286  
287  
288  
289  
290  
291  
292  
293  
294  
295  
296  
297  
298  
299  
300  
301  
302  
303  
304  
305  
306  
307  
308  
309  
310  
311  
312  
313  
314  
315  
316  
317  
318  
319  
320  
321  
322  
323  
324  
325  
326  
327  
328  
329  
330  
331  
332  
333  
334  
335  
336  
337  
338  
339  
340  
341  
342  
343  
344  
345  
346  
347  
348  
349  
350  
351  
352  
353  
354  
355  
356  
357  
358  
359  
360  
361  
362  
363  
364  
365  
366  
367  
368  
369  
370  
371  
372  
373  
374  
375  
376  
377  
378  
379  
380  
381  
382  
383  
384  
385  
386  
387  
388  
389  
390  
391  
392  
393  
394  
395  
396  
397  
398  
399  
400  
401  
402  
403  
404  
405  
406  
407  
408  
409  
410  
411  
412  
413  
414  
415  
416  
417  
418  
419  
420  
421  
422  
423  
424  
425  
426  
427  
428  
429  
430  
431  
432  
433  
434  
435  
436  
437  
438  
439  
440  
441  
442  
443  
444  
445  
446  
447  
448  
449  
450  
451  
452  
453  
454  
455  
456  
457  
458  
459  
460  
461  
462  
463  
464  
465  
466  
467  
468  
469  
470  
471  
472  
473  
474  
475  
476  
477  
478  
479  
480  
481  
482  
483  
484  
485  
486  
487  
488  
489  
490  
491  
492  
493  
494  
495  
496  
497  
498  
499  
500  
501  
502  
503  
504  
505  
506  
507  
508  
509  
510  
511  
512  
513  
514  
515  
516  
517  
518  
519  
520  
521  
522  
523  
524  
525  
526  
527  
528  
529  
530  
531  
532  
533  
534  
535  
536  
537  
538  
539  
540  
541  
542  
543  
544  
545  
546  
547  
548  
549  
550  
551  
552  
553  
554  
555  
556  
557  
558  
559  
560  
561  
562  
563  
564  
565  
566  
567  
568  
569  
570  
571  
572  
573  
574  
575  
576  
577  
578  
579  
580  
581  
582  
583  
584  
585  
586  
587  
588  
589  
590  
591  
592  
593  
594  
595  
596  
597  
598  
599  
600  
601  
602  
603  
604  
605  
606  
607  
608  
609  
610  
611  
612  
613  
614  
615  
616  
617  
618  
619  
620  
621  
622  
623  
624  
625  
626  
627  
628  
629  
630  
631  
632  
633  
634  
635  
636  
637  
638  
639  
640  
641  
642  
643  
644  
645  
646  
647  
648  
649  
650  
651  
652  
653  
654  
655  
656  
657  
658  
659  
660  
661  
662  
663  
664  
665  
666  
667  
668  
669  
670  
671  
672  
673  
674  
675  
676  
677  
678  
679  
680  
681  
682  
683  
684  
685  
686  
687  
688  
689  
690  
691  
692  
693  
694  
695  
696  
697  
698  
699  
700  
701  
702  
703  
704  
705  
706  
707  
708  
709  
710  
711  
712  
713  
714  
715  
716  
717  
718  
719  
720  
721  
722  
723  
724  
725  
726  
727  
728  
729  
730  
731  
732  
733  
734  
735  
736  
737  
738  
739  
740  
741  
742  
743  
744  
745  
746  
747  
748  
749  
750  
751  
752  
753  
754  
755  
756  
757  
758  
759  
760  
761  
762  
763  
764  
765  
766  
767  
768  
769  
770  
771  
772  
773  
774  
775  
776  
777  
778  
779  
780  
781  
782  
783  
784  
785  
786  
787  
788  
789  
790  
791  
792  
793  
794  
795  
796  
797  
798  
799  
800  
801  
802  
803  
804  
805  
806  
807  
808  
809  
810  
811  
812  
813  
814  
815  
816  
817  
818  
819  
820  
821  
822  
823  
824  
825  
826  
827  
828  
829  
830  
831  
832  
833  
834  
835  
836  
837  
838  
839  
840  
841  
842  
843  
844  
845  
846  
847  
848  
849  
850  
851  
852  
853  
854  
855  
856  
857  
858  
859  
860  
861  
862  
863  
864  
865  
866  
867  
868  
869  
870  
871  
872  
873  
874  
875  
876  
877  
878  
879  
880  
881  
882  
883  
884  
885  
886  
887  
888  
889  
890  
891  
892  
893  
894  
895  
896  
897  
898  
899  
900  
901  
902  
903  
904  
905  
906  
907  
908  
909  
910  
911  
912  
913  
914  
915  
916  
917  
918  
919  
920  
921  
922  
923  
924  
925  
926  
927  
928  
929  
930  
931  
932  
933  
934  
935  
936  
937  
938  
939  
940  
941  
942  
943  
944  
945  
946  
947  
948  
949  
950  
951  
952  
953  
954  
955  
956  
957  
958  
959  
960  
961  
962  
963  
964  
965  
966  
967  
968  
969  
970  
971  
972  
973  
974  
975  
976  
977  
978  
979  
980  
981  
982  
983  
984  
985  
986  
987  
988  
989  
990  
991  
992  
993  
994  
995  
996  
997  
998  
999  
1000

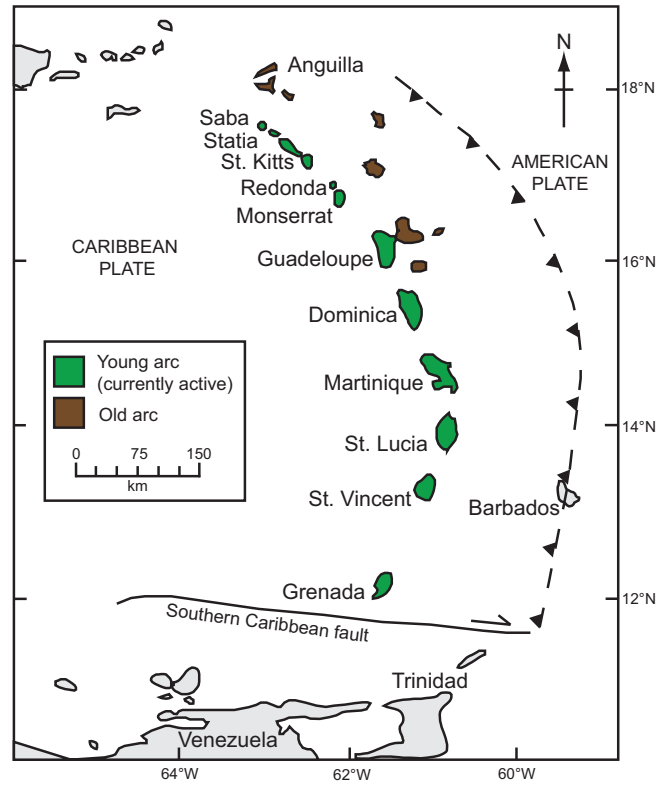
999  
1000  
1001  
1002  
1003  
1004  
1005  
1006  
1007  
1008  
1009  
1010  
1011  
1012  
1013  
1014  
1015  
1016  
1017  
1018  
1019  
1020  
1021  
1022  
1023  
1024  
1025  
1026  
1027  
1028  
1029  
1030  
1031  
1032  
1033  
1034  
1035  
1036  
1037  
1038  
1039  
1040  
1041  
1042  
1043  
1044  
1045  
1046  
1047  
1048  
1049  
1050  
1051  
1052  
1053  
1054  
1055  
1056  
1057  
1058  
1059  
1060  
1061  
1062  
1063  
1064  
1065  
1066  
1067  
1068  
1069  
1070  
1071  
1072  
1073  
1074  
1075  
1076  
1077  
1078  
1079  
1080  
1081  
1082  
1083  
1084  
1085  
1086  
1087  
1088  
1089  
1090  
1091  
1092  
1093  
1094  
1095  
1096  
1097  
1098  
1099  
1100  
1101  
1102  
1103  
1104  
1105  
1106  
1107  
1108  
1109  
1110  
1111  
1112  
1113  
1114  
1115  
1116  
1117  
1118  
1119  
1120  
1121  
1122  
1123  
1124  
1125  
1126  
1127  
1128  
1129  
1130  
1131  
1132  
1133  
1134  
1135  
1136  
1137  
1138  
1139  
1140  
1141  
1142  
1143  
1144  
1145  
1146  
1147  
1148  
1149  
1150  
1151  
1152  
1153  
1154  
1155  
1156  
1157  
1158  
1159  
1160  
1161  
1162  
1163  
1164  
1165  
1166  
1167  
1168  
1169  
1170  
1171  
1172  
1173  
1174  
1175  
1176  
1177  
1178  
1179  
1180  
1181  
1182  
1183  
1184  
1185  
1186  
1187  
1188  
1189  
1190  
1191  
1192  
1193  
1194  
1195  
1196  
1197  
1198  
1199  
1200  
1201  
1202  
1203  
1204  
1205  
1206  
1207  
1208  
1209  
1210  
1211  
1212  
1213  
1214  
1215  
1216  
1217  
1218  
1219  
1220  
1221  
1222  
1223  
1224  
1225  
1226  
1227  
1228  
1229  
1230  
1231  
1232  
1233  
1234  
1235  
1236  
1237  
1238  
1239  
1240  
1241  
1242  
1243  
1244  
1245  
1246  
1247  
1248  
1249  
1250  
1251  
1252  
1253  
1254  
1255  
1256  
1257  
1258  
1259  
1260  
1261  
1262  
1263  
1264  
1265  
1266  
1267  
1268  
1269  
1270  
1271  
1272  
1273  
1274  
1275  
1276  
1277  
1278  
1279  
1280  
1281  
1282  
1283  
1284  
1285  
1286  
1287  
1288  
1289  
1290  
1291  
1292  
1293  
1294  
1295  
1296  
1297  
1298  
1299  
1300  
1301  
1302  
1303  
1304  
1305  
1306  
1307  
1308  
1309  
1310  
1311  
1312  
1313  
1314  
1315  
1316  
1317  
1318  
1319  
1320  
1321  
1322  
1323  
1324  
1325  
1326  
1327  
1328  
1329  
1330  
1331  
1332  
1333  
1334  
1335  
1336  
1337  
1338  
1339  
1340  
1341  
1342  
1343  
1344  
1345  
1346  
1347  
1348  
1349  
1350  
1351  
1352  
1353  
1354  
1355  
1356  
1357  
1358  
1359  
1360  
1361  
1362  
1363  
1364  
1365  
1366  
1367  
1368  
1369  
1370  
1371  
1372  
1373  
1374  
1375  
1376  
1377  
1378  
1379  
1380  
1381  
1382  
1383  
1384  
1385  
1386  
1387  
1388  
1389  
1390  
1391  
1392  
1393  
1394  
1395  
1396  
1397  
1398  
1399  
1400  
1401  
1402  
1403  
1404  
1405  
1406  
1407  
1408  
1409  
1410  
1411  
1412  
1413  
1414  
1415  
1416  
1417  
1418  
1419  
1420  
1421  
1422  
1423  
1424  
1425  
1426  
1427  
1428  
1429  
1430  
1431  
1432  
1433  
1434  
1435  
1436  
1437  
1438  
1439  
1440  
1441  
1442  
1443  
1444  
1445  
1446  
1447  
1448  
1449  
1450  
1451  
1452  
1453  
1454  
1455  
1456  
1457  
1458  
1459  
1460  
1461  
1462  
1463  
1464  
1465  
1466  
1467  
1468  
1469  
1470  
1471  
1472  
1473  
1474  
1475  
1476  
1477  
1478  
1479  
1480  
1481  
1482  
1483  
1484  
1485  
1486  
1487  
1488  
1489  
1490  
1491  
1492  
1493  
1494  
1495  
1496  
1497  
1498  
1499  
1500  
1501  
1502  
1503  
1504  
1505  
1506  
1507  
1508  
1509  
1510  
1511  
1512  
1513  
1514  
1515  
1516  
1517  
1518  
1519  
1520  
1521  
1522  
1523  
1524  
1525  
1526  
1527  
1528  
1529  
1530  
1531  
1532  
1533  
1534  
1535  
1536  
1537  
1538  
1539  
1540  
1541  
1542  
1543  
1544  
1545  
1546  
1547  
1548  
1549  
1550  
1551  
1552  
1553  
1554  
1555  
1556  
1557  
1558  
1559  
1560  
1561  
1562  
1563  
1564  
1565  
1566  
1567  
1568  
1569  
1570  
1571  
1572  
1573  
1574  
1575  
1576  
1577  
1578  
1579  
1580  
1581  
1582  
1583  
1584  
1585  
1586  
1587  
1588  
1589  
1590  
1591  
1592  
1593  
1594  
1595  
1596  
1597  
1598  
1599  
1600  
1601  
1602  
1603  
1604  
1605  
1606  
1607  
1608  
1609  
1610  
1611  
1612  
1613  
1614  
1615  
1616  
1617  
1618  
1619  
1620  
1621  
1622  
1623  
1624  
1625  
1626  
1627  
1628  
1629  
1630  
1631  
1632  
1633  
1634  
1635  
1636  
1637  
1638  
1639  
1640  
1641  
1642  
1643  
1644  
1645  
1646  
1647  
1648  
1649  
1650  
1651  
1652  
1653  
1654  
1655  
1656  
1657  
1658  
1659  
1660  
1661  
1662  
1663  
1664  
1665  
1666  
1667  
1668  
1669  
1670  
1671  
1672  
1673  
1674  
1675  
1676  
1677  
1678  
1679  
1680  
1681  
1682  
1683  
1684  
1685  
1686  
1687  
1688  
1689  
1690  
1691  
1692  
1693  
1694  
1695  
1696  
1697  
1698  
1699  
1700  
1701  
1702  
1703  
1704  
1705  
1706  
1707  
1708  
1709  
1710  
1711  
1712  
1713  
1714  
1715  
1716  
1717  
1718  
1719  
1720  
1721  
1722  
1723  
1724  
1725  
1726  
1727  
1728  
1729  
1730  
1731  
1732  
1733  
1734  
1735  
1736  
1737  
1738  
1739  
1740  
1741  
1742  
1743  
1744  
1745  
1746  
1747  
1748  
1749  
1750  
1751  
1752  
1753  
1754  
1755  
1756  
1757  
1758  
1759  
1760  
1761  
1762  
1763  
1764  
1765  
1766  
1767  
1768  
1769  
1770  
1771  
1772  
1773  
1774  
1775  
1776  
1777  
1778  
1779  
1780  
1781  
1782  
1783  
1784  
1785  
1786  
1787  
1788  
1789  
1790  
1791  
1792  
1793  
1794  
1795  
1796  
1797  
1798  
1799  
1800  
1801  
1802  
1803  
1804  
1805  
1806  
1807  
1808  
1809  
1810  
1811  
1812  
1813  
1814  
1815  
1816  
1817  
1818  
1819  
1820  
1821  
1822  
1823  
1824  
1825  
1826  
1827  
1828  
1829  
1830  
1831  
1832  
1833  
1834  
1835  
1836  
1837  
1838  
1839  
1840  
1841  
1842  
1843  
1844  
1845  
1846  
1847  
1848  
1849  
1850  
1851  
1852  
1853  
1854  
1855  
1856  
1857  
1858  
1859  
1860  
1861  
1862  
1863  
1864  
1865  
1866  
1867  
1868  
1869  
1870  
1871  
1872  
1873  
1874  
1875  
1876  
1877  
1878  
1879  
1880  
1881  
1882  
1883  
1884  
1885  
1886  
1887  
1888  
1889  
1890  
1891  
1892  
1893  
1894  
1895  
1896  
1897  
1898  
1899  
1900  
1901  
1902  
1903  
1904  
1905  
1906  
1907  
1908  
1909  
1910  
1911  
1912  
1913  
1914  
1915  
1916  
1917  
1918  
1919  
1920  
1921  
1922  
1923  
1924  
1925  
1926  
1927  
1928  
1929  
1930  
1931  
1932  
1933  
1934  
1935  
1936  
1937  
1938  
1939  
1940  
1941  
1942  
1943  
1944  
1945  
1946  
1947  
1948  
1949  
1950  
1951  
1952  
1953  
1954  
1955  
1956  
1957  
1958  
1959  
1960  
1961  
1962  
1963  
1964  
1965  
1966  
1967  
1968  
1969  
1970  
1971  
1972  
1973  
1974  
1975  
1976  
1977  
1978  
1979  
1980  
1981  
1982  
1983  
1984  
1985  
1986  
1987  
1988  
1989  
1990  
1991  
1992  
1993  
1994  
1995  
1996  
1997  
1998  
1999  
2000  
2001  
2002  
2003  
2004  
2005  
2006  
2007  
2008  
2009  
2010  
2011  
2012  
2013  
2014  
2015  
2016  
2017  
2018  
2019  
2020  
2021  
2022  
2023  
2024  
2025  
2026  
2027  
2028  
2029  
2030  
2031  
2032  
2033  
2034  
2035  
2036  
2037  
2038  
2039  
2040  
2041  
2042  
2043  
2044  
2045  
2046  
2047  
2048  
2049  
2050  
2051  
2052  
2053  
2054  
2055  
2056  
2057  
2058  
2059  
2060  
2061  
2062  
2063  
2064  
2065  
2066  
2067  
2068  
2069  
2070  
2071  
2072  
2073  
2074  
2075  
2076  
2077  
2078  
2079  
2080  
2081  
2082  
2083  
2084  
2085  
2086  
2087  
2088  
2089  
2090  
2091  
2092  
2093  
2094  
2095  
2096  
2097  
2098  
2099  
2100  
2101  
2102  
2103  
2104  
2105  
2106  
2107  
2108  
2109  
2110  
2111  
2112  
2113  
2114  
2115  
2116  
2117  
2118  
2119  
21

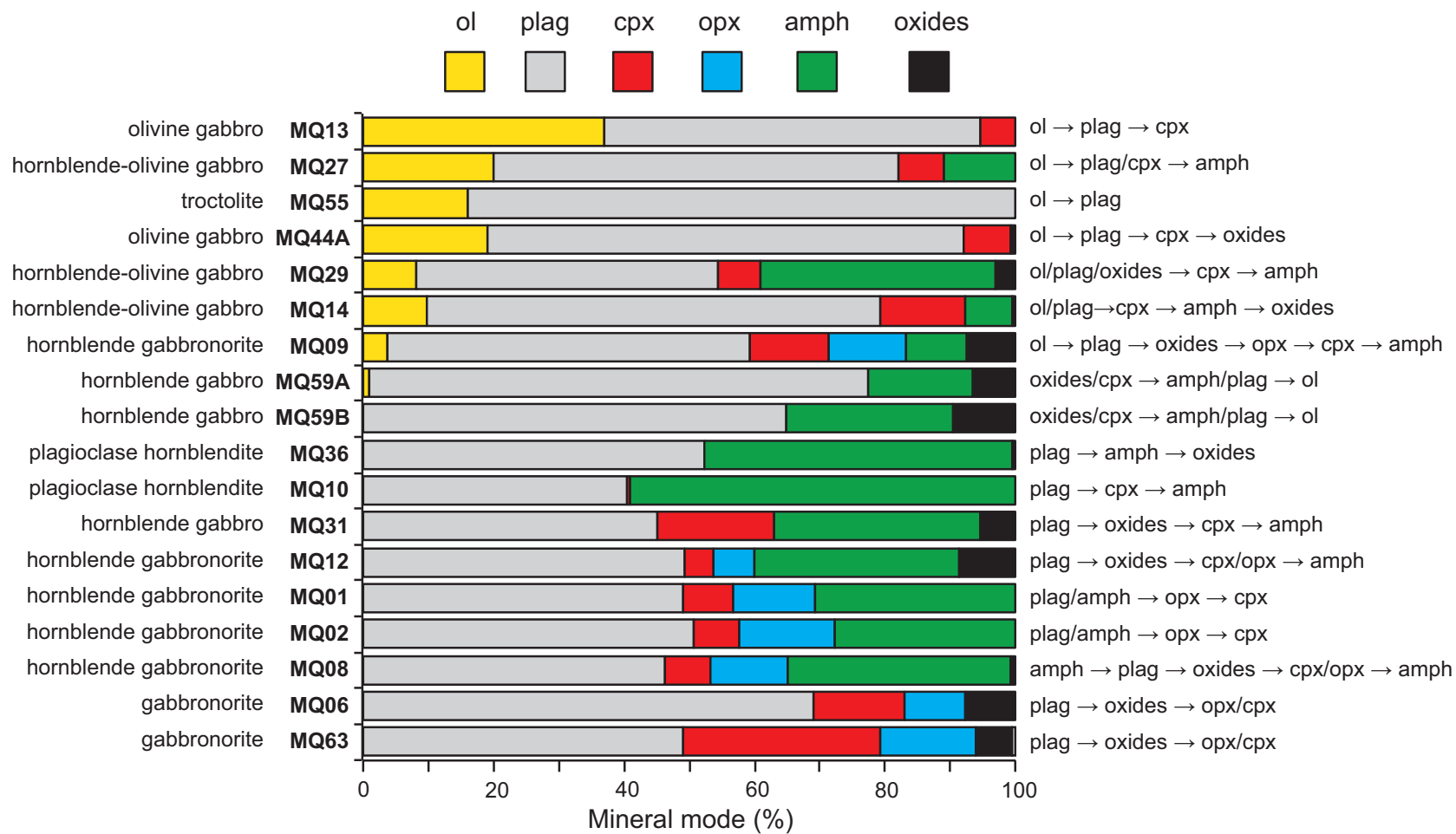
1 Wadge G, Shepherd J (1984) Segmentation of the Lesser Antilles subduction zone. Earth and  
2 Planetary Science Letters 71(2):297-304  
3

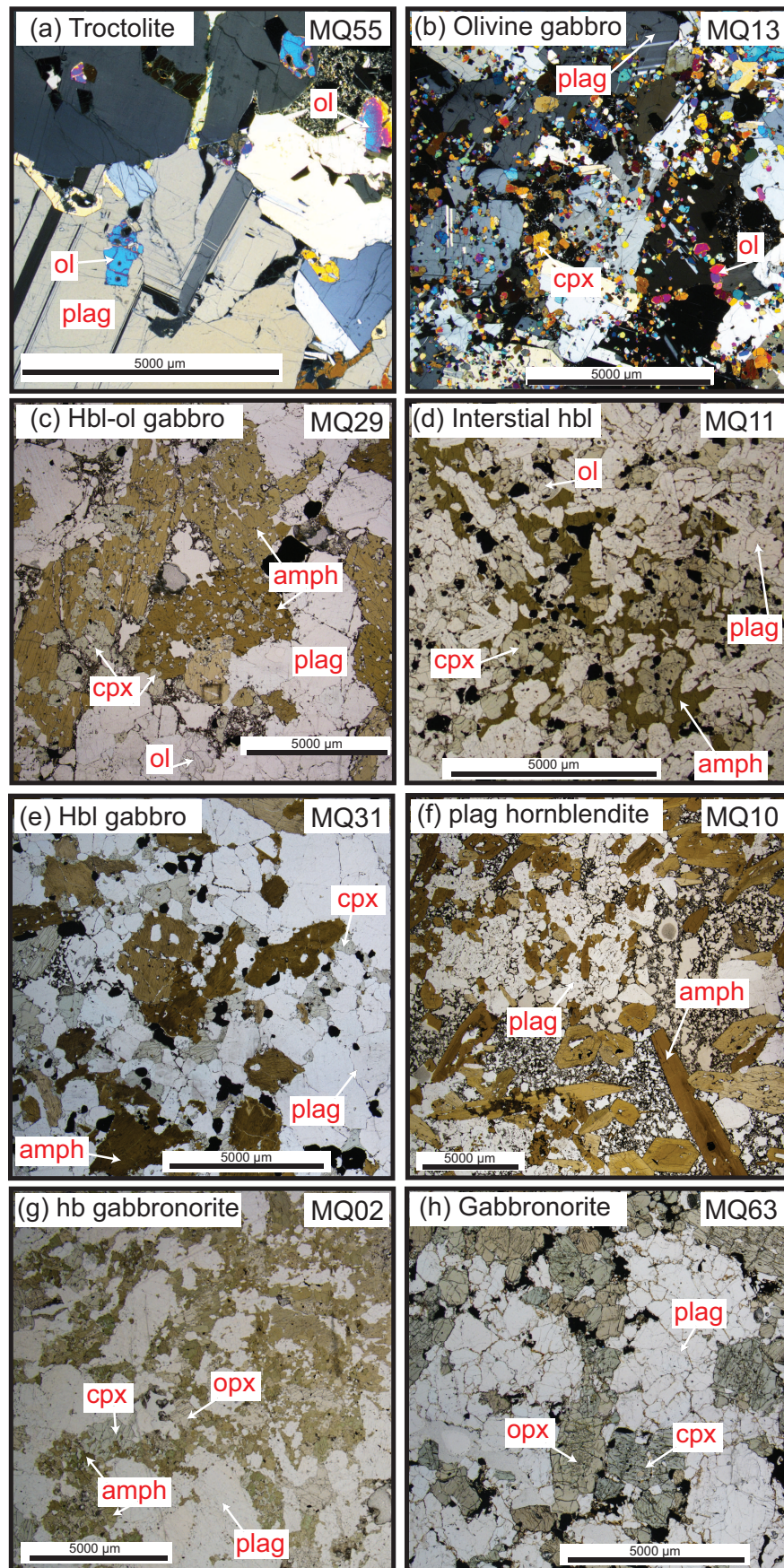
4  
5 Wager LR, Brown GM, Wadsworth WJ (1960) Types of igneous cumulates. Journal of  
6 Petrology 1:73-85  
7

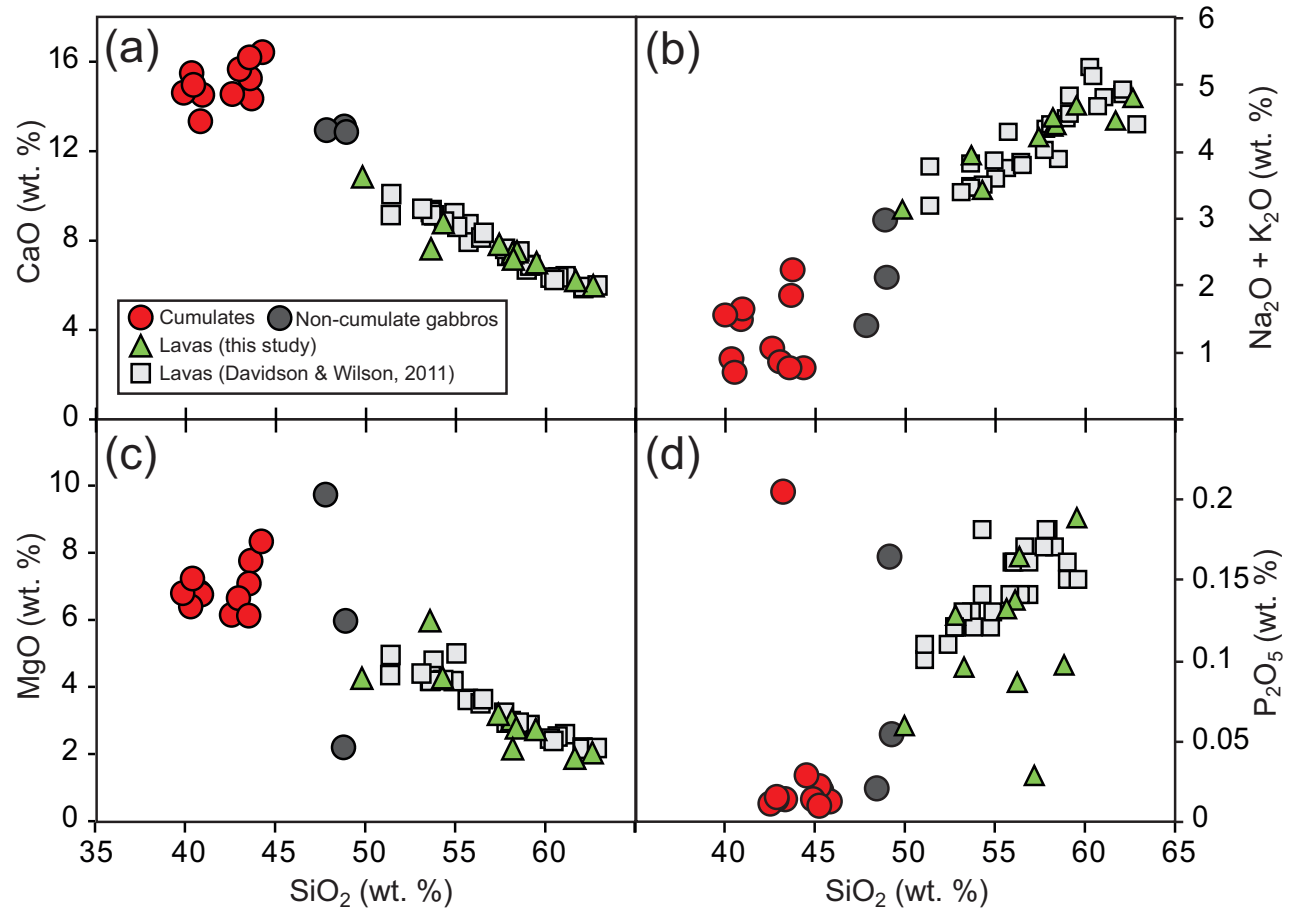
8  
9  
10  
11 Westercamp D, Andreieff P, Bouysse P, Cottez S, Battistini R (1989). Martinique. Carte  
12 geologique a' 1/50 000. Orleans: BRGM  
13

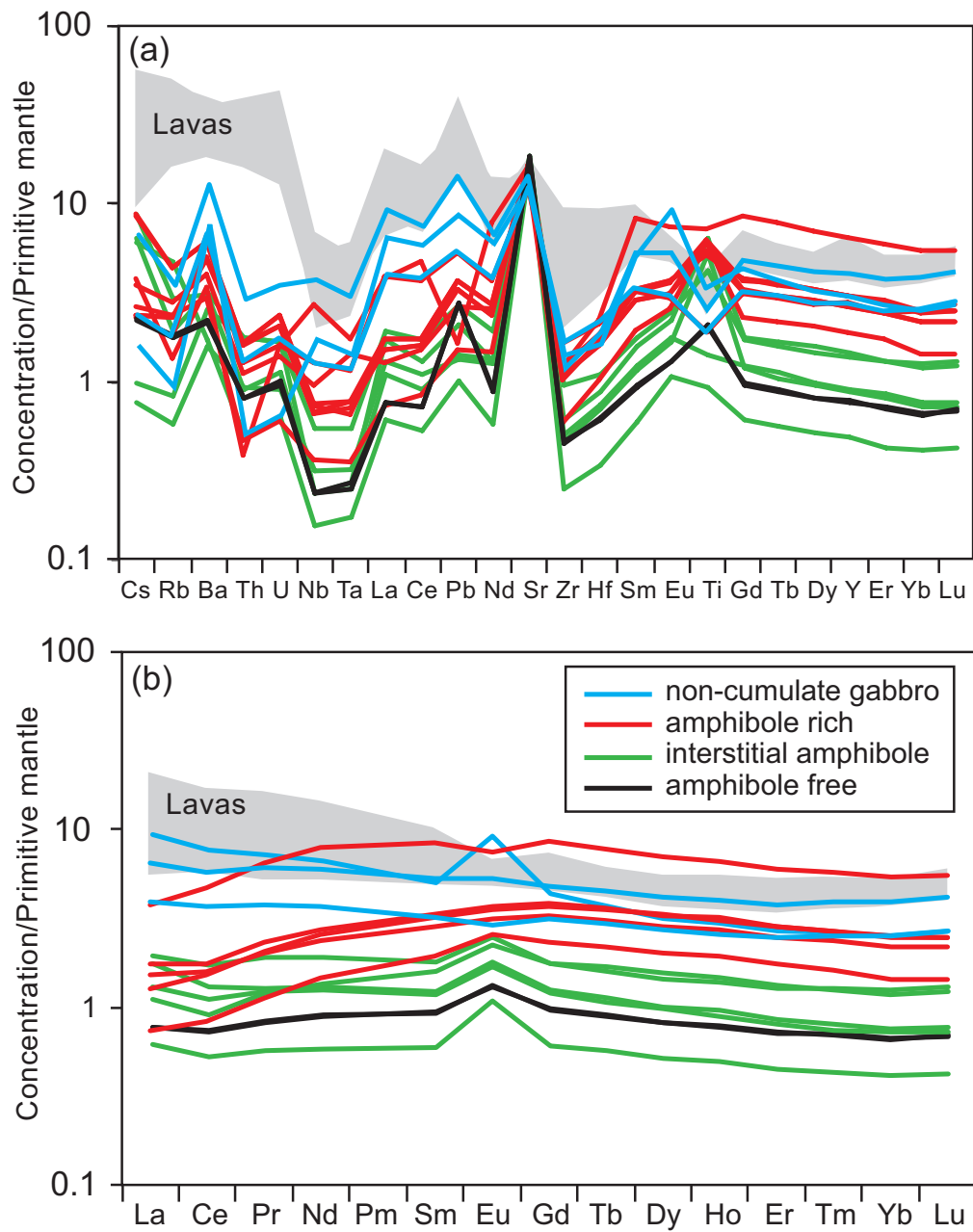
14  
15  
16  
17 Wood BJ, Blundy JD (1997) A predictive model for rare earth element partitioning between  
18 clinopyroxene and anhydrous silicate melt. Contributions to Mineralogy and Petrology 129(2-  
19 3):166-181 doi:10.1007/s004100050330  
20  
21  
22  
23  
24  
25  
26  
27  
28  
29  
30  
31  
32  
33  
34  
35  
36  
37  
38  
39  
40  
41  
42  
43  
44  
45  
46  
47  
48  
49  
50  
51  
52  
53  
54  
55  
56  
57  
58  
59  
60  
61  
62  
63  
64  
65

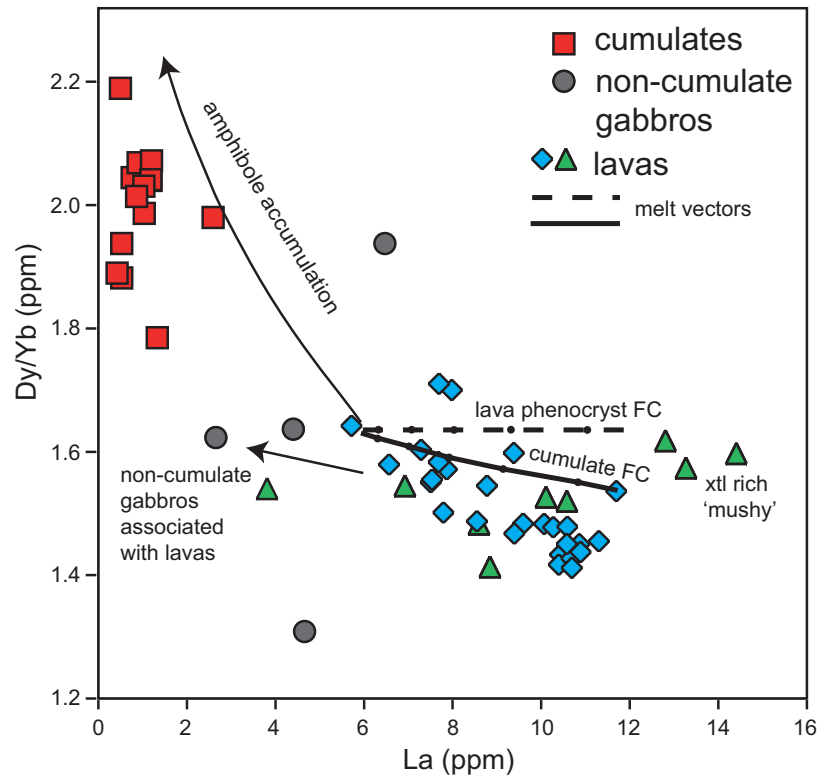


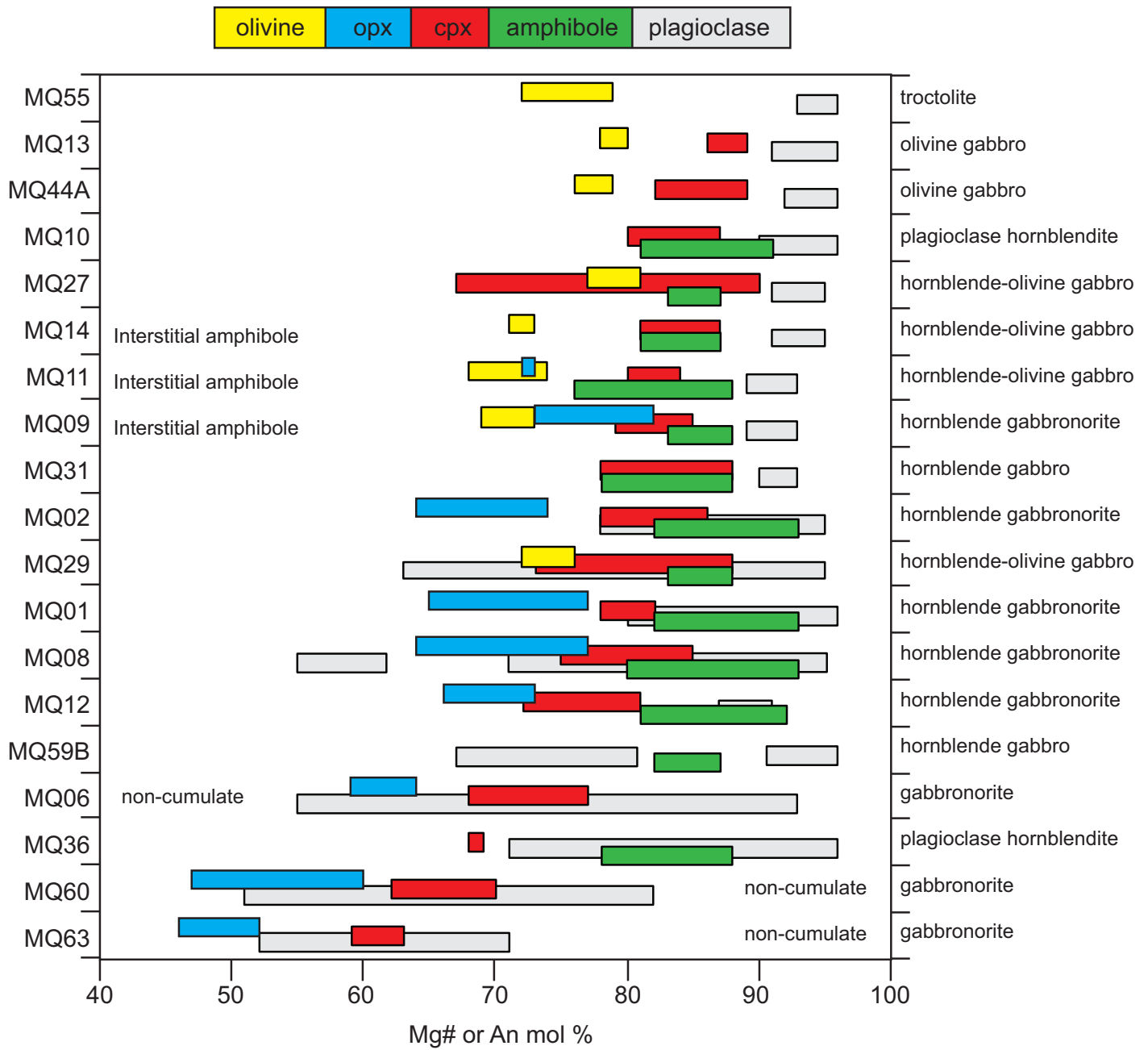


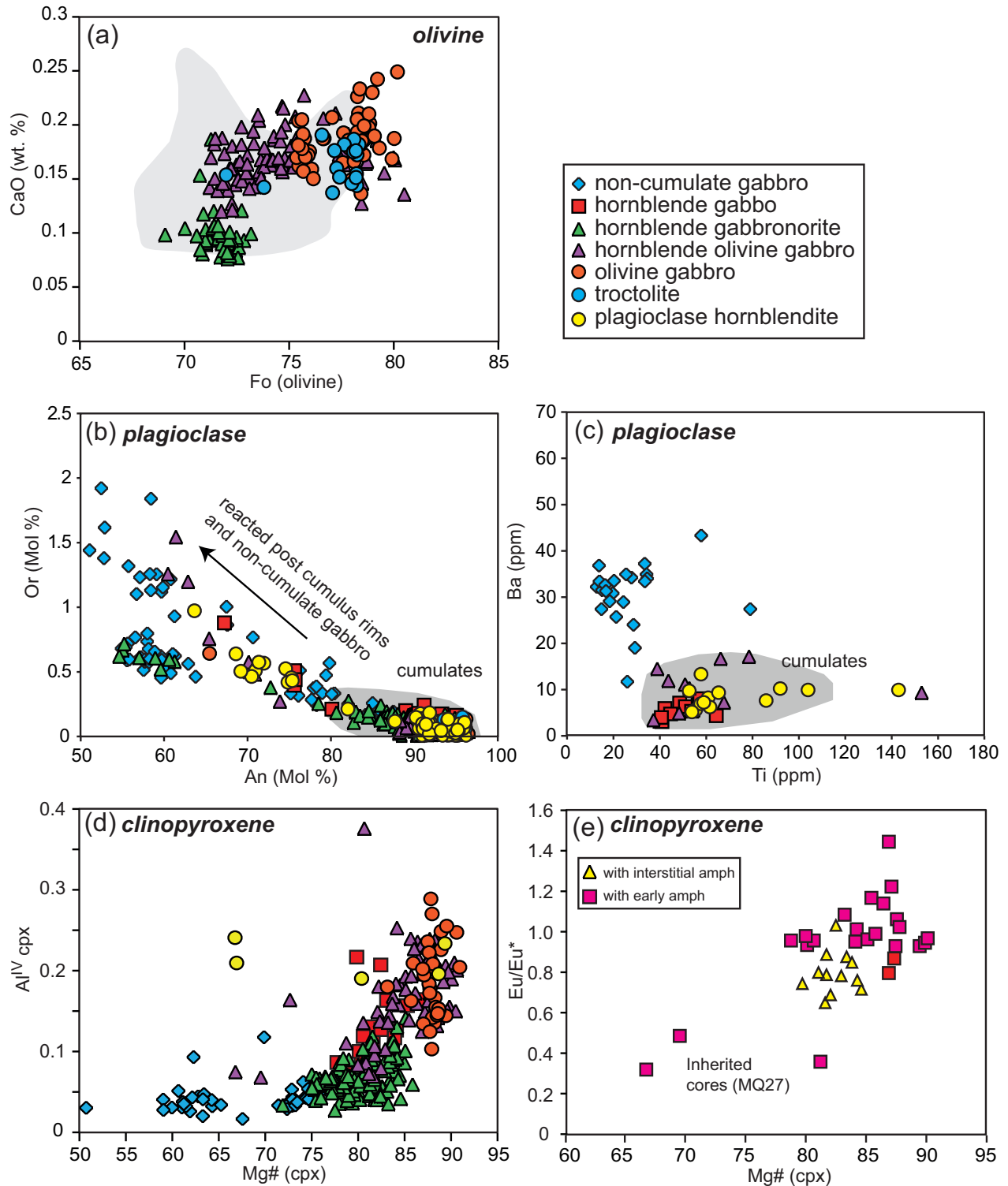


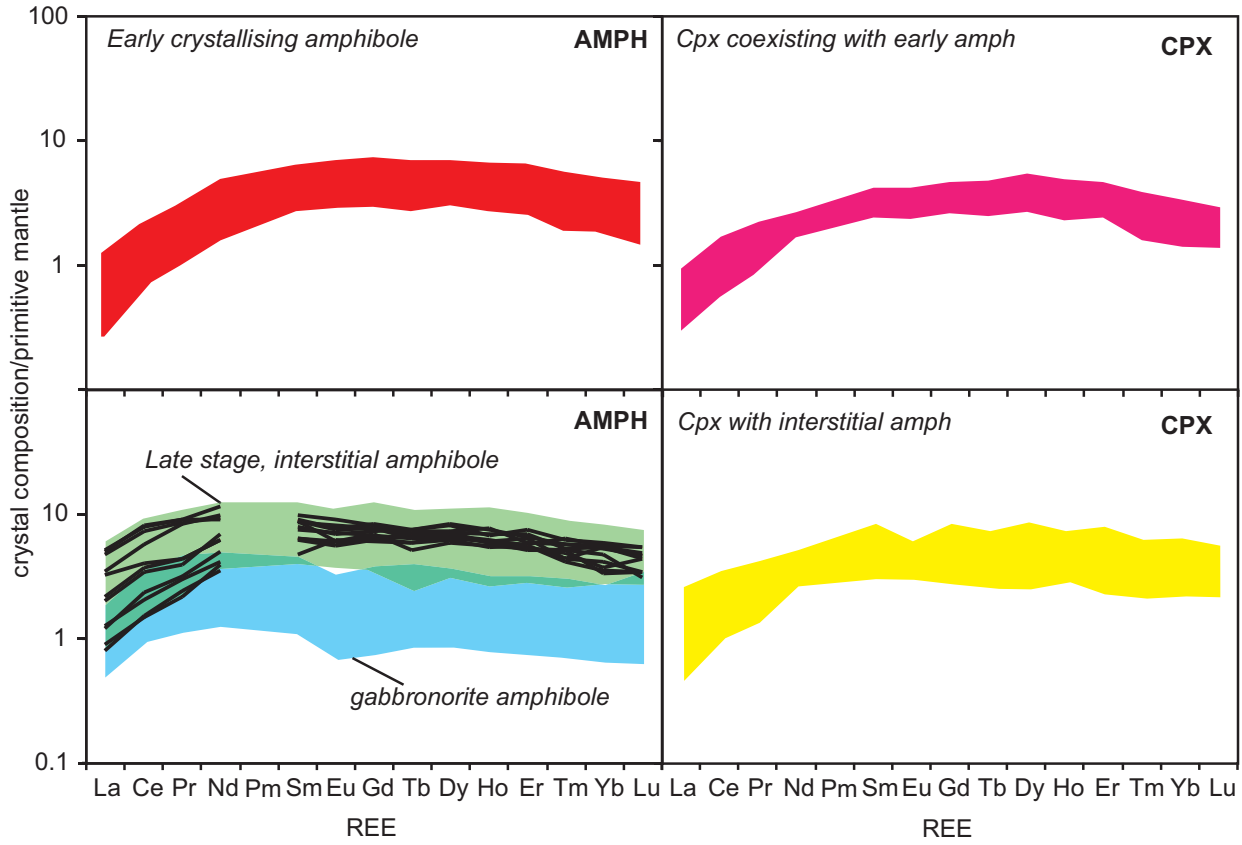


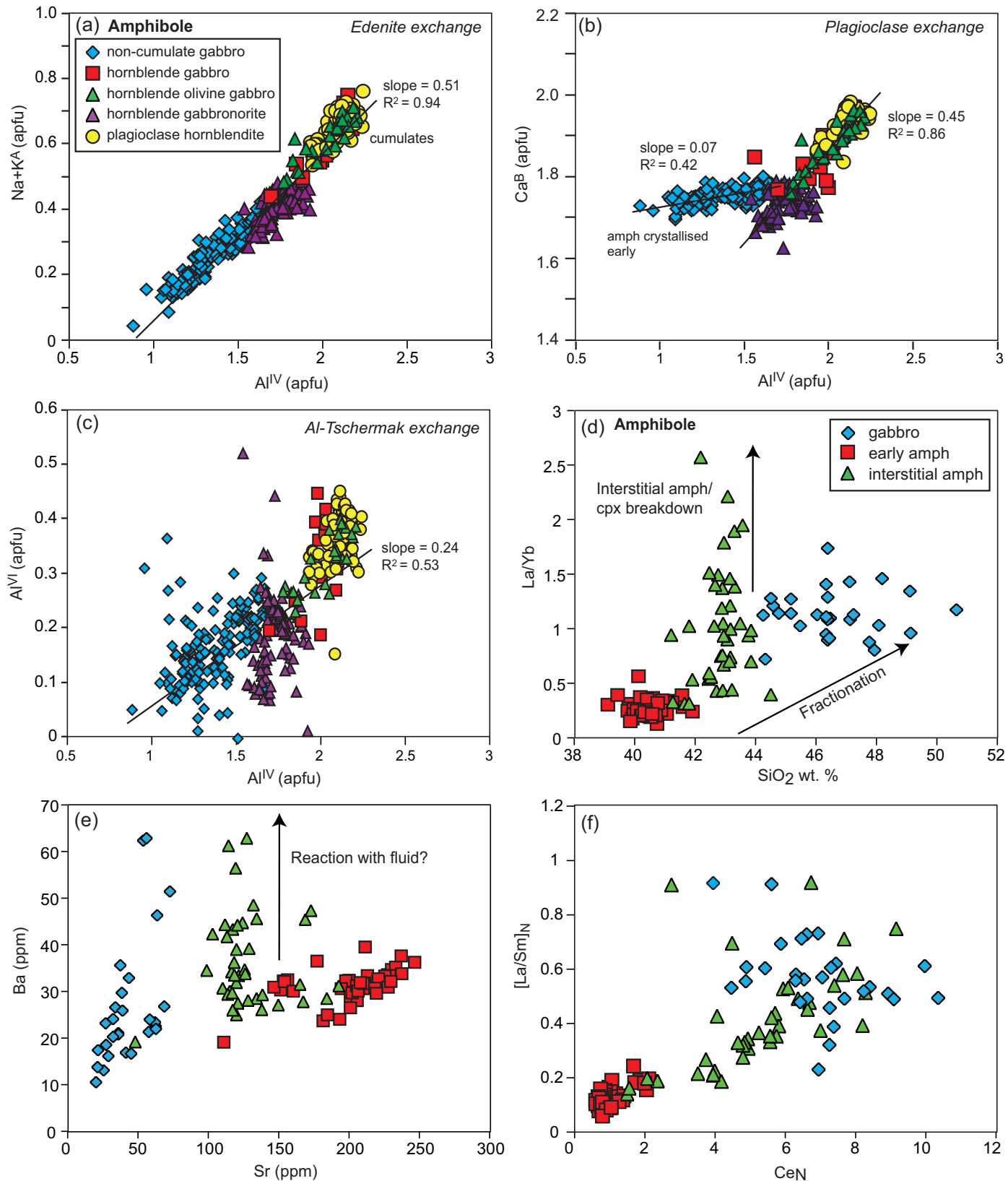


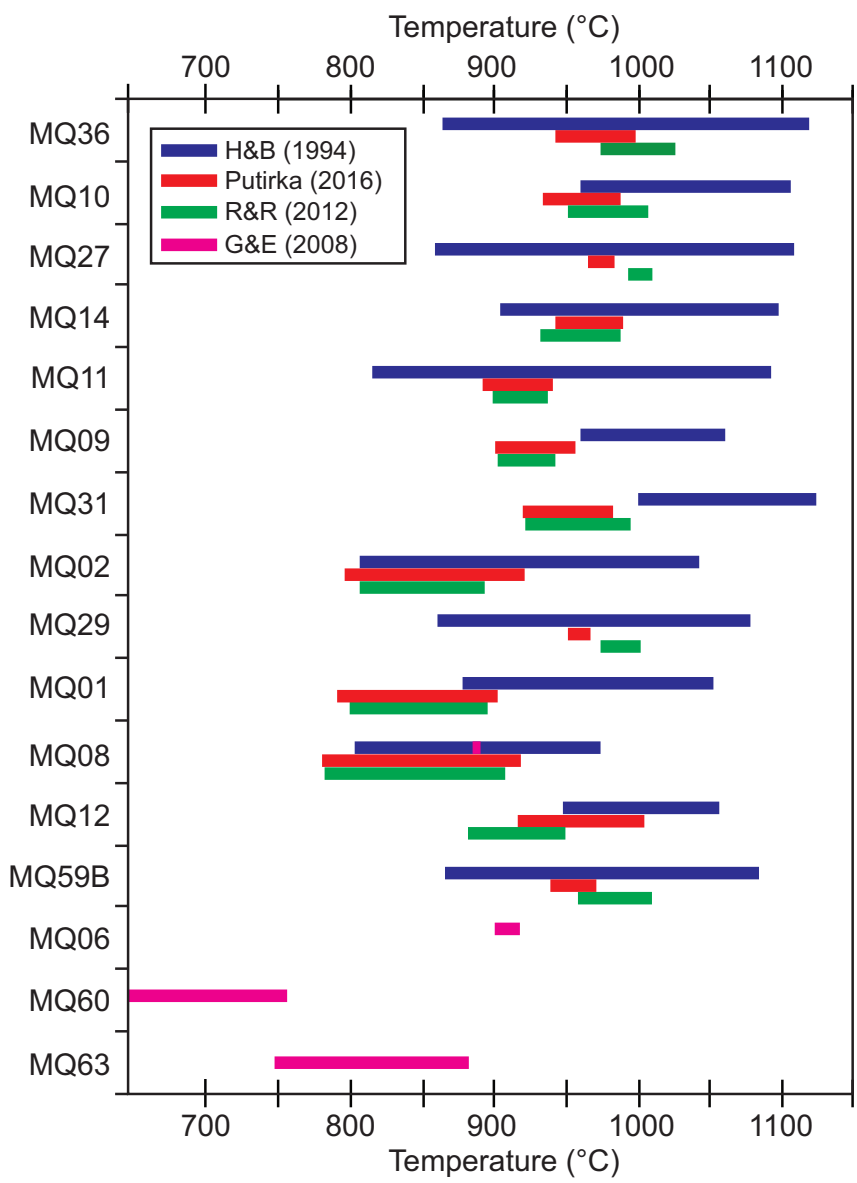


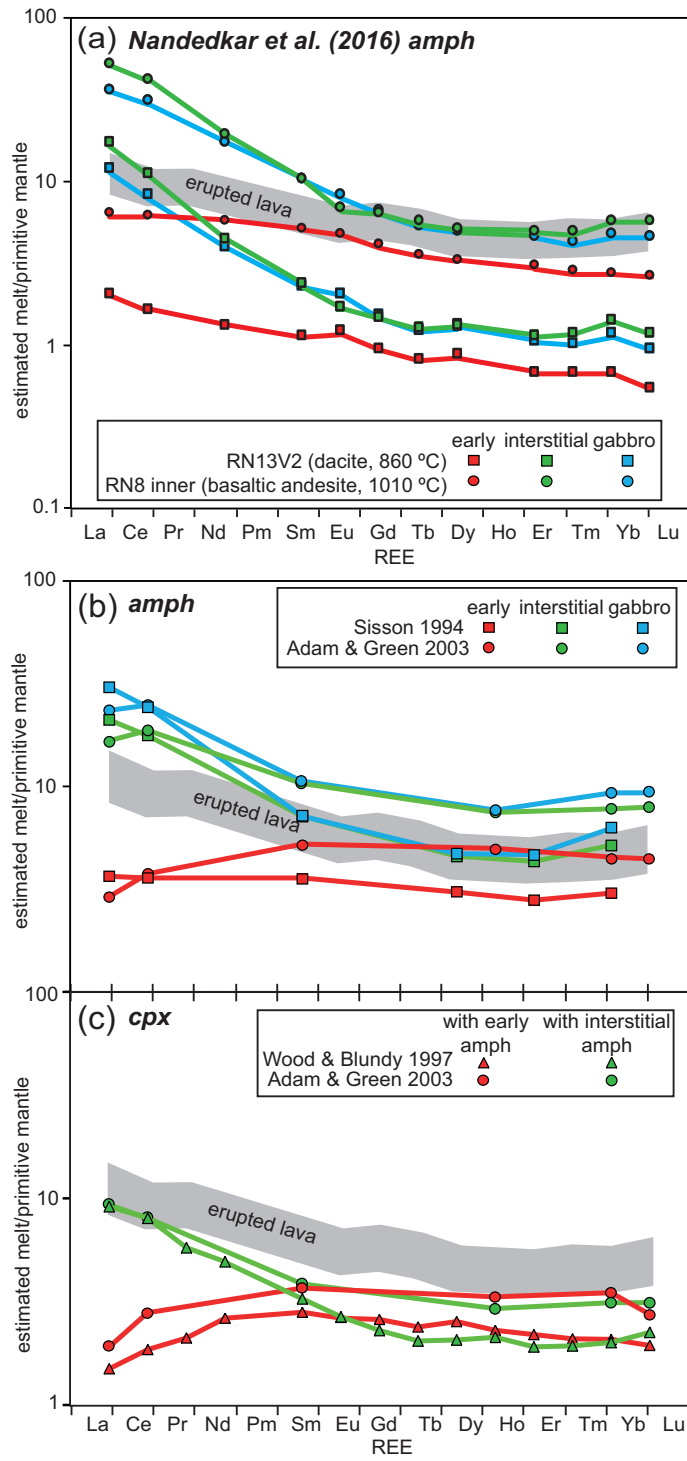












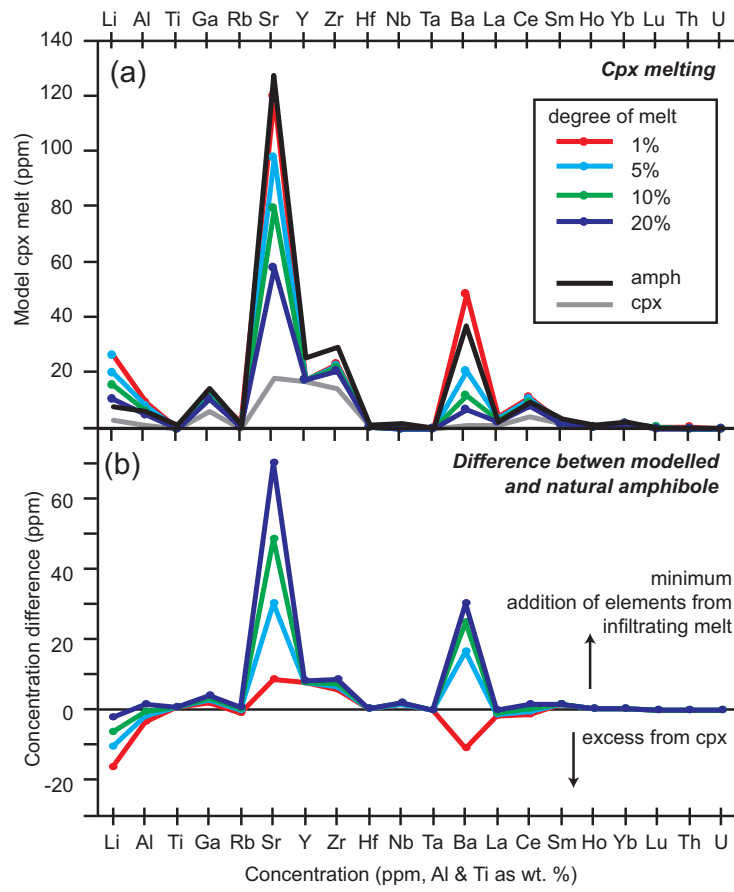


**Table 1.** Comparison of appropriate experimental studies which return assemblages and compositions close to that of the natural plutonic xenolith samples.

	<b>Experiment</b>	<b>Compositions</b>		<b>Temperature</b>	<b>Pressure</b>	<b>H<sub>2</sub>O</b>
<b>Troctolite/olivine gabbro</b>	Sisson & Grove (1993)-Low Mg-high Al basalt	olivine Fo 72-80	cpx ~0.1 Al <sup>IV</sup>	1020-1082 °C	0.1 GPa	Saturated
	Pichavant & MacDonald (2007)-High Al basalt	olivine Fo 75-82	cpx ~0.2 Al <sup>IV</sup>	1050-1150 °C	0.4 GPa	1.7-5.9 wt. %
<b>Plagioclase hornblendite</b>	Pichavant et al. (2002)-Basaltic Andesite	plag An 75-90	hbl ~ 1.7 Al <sup>IV</sup>	945-949 °C	0.4 GPa	8.2 wt. %
<b>Hornbende gabbro</b>	Pichavant et al. (2002)-Basaltic Andesite	olivine Fo 70 plag An 85	hbl ~ 1.8 Al <sup>IV</sup> cpx ~0.15 Al <sup>IV</sup>	1000 °C	0.4 GPa	6.8 wt. %
	Sisson & Grove (1993)-High Al basalt	olivine Fo 77 plag An 85	hbl ~ 1.8 Al <sup>IV</sup> cpx ~0.23 Al <sup>IV</sup>	965 °C	0.2 GPa	Saturated
<b>(Hornblende) gabbronorite</b>	Pichavant et al. (2002)-Basaltic Andesite	plag An 62-71	cpx En 35-54 opx En 54-82	950-1016 °C	0.4 GPa	3.9-6.9 wt. %
	Melekhova et al. (2015)-High MgO basalt	Plag An 47-81 hbl 1.75-2.1 Al <sup>IV</sup>	cpx En 44-46 opx En 77-86	950-1230 °C	0.7-1 GPa	0.6-2.3 wt. %